Physical Drivers of Southwest African Coastal Upwelling and Its Response to Climate Variability and Change

9

Peter Brandt, Mohammad Hadi Bordbar, Paulo Coelho, Rodrigue Anicet Imbol Koungue, Mareike Körner, Tarron Lamont, Joke F. Lübbecke, Volker Mohrholz, Arthur Prigent, Marisa Roch, Martin Schmidt, Anja K. van der Plas, and Jennifer Veitch (iD)

P. Brandt (✉)
GEOMAR Helmholtz Centre for Ocean Research Kiel, Kiel, Germany

Faculty of Mathematics and Natural Sciences, Kiel University, Kiel, Germany
e-mail: pbrandt@geomar.de

M. H. Bordbar · V. Mohrholz · M. Schmidt
Leibniz Institute for Baltic Sea Research Warnemünde, Rostock, Germany
e-mail: hadi.bordbar@io-warnemuende.de; volker.mohrholz@io-warnemuende.de;
martin.schmidt@io-warnemuende.de

P. Coelho
Instituto Nacional de Investigação Pesqueira e Marinha, Ministério da Agricultura e Pescas de Angola, Ilha de Luanda, Luanda, Angola

R. A. Imbol Koungue · M. Körner · J. F. Lübbecke · A. Prigent · M. Roch
GEOMAR Helmholtz Centre for Ocean Research Kiel, Kiel, Germany
e-mail: rimbol@geomar.de; mkoerner@geomar.de; jluebbecke@geomar.de;
aprigent@geomar.de; mroch@geomar.de

T. Lamont
Oceans & Coasts Research Branch, Department of Forestry, Fisheries, and the Environment, Cape Town, South Africa

Department of Oceanography, University of Cape Town, Rondebosch, South Africa

Bayworld Centre for Research & Education, Cape Town, South Africa
e-mail: tlamont@dffe.gov.za

A. K. van der Plas
National Marine Information and Research Centre, Ministry of Fisheries and Marine Resources, Swakopmund, Namibia; Anja.VanDerPlas@mfmr.gov.na

J. Veitch
The South African Environmental Observation Network, Cape Town, South Africa
e-mail: ja.veitch@saeon.nrf.ac.za

221

Abstract

The southeastern tropical Atlantic hosts a coastal upwelling system characterized by high biological productivity. Three subregions can be distinguished based on differences in the physical climate: the tropical Angolan and the northern and southern Benguela upwelling systems (tAUS, nBUS, sBUS). The tAUS, which is remotely forced via equatorial and coastal trapped waves, can be characterized as a mixing-driven system, where the wind forcing plays only a secondary role. The nBUS and sBUS are both forced by alongshore winds and offshore cyclonic wind stress curl. While the nBUS is a permanent upwelling system, the sBUS is impacted by the seasonal cycle of alongshore winds. Interannual variability in the region is dominated by Benguela Niños and Niñas that are warm and cold events observed every few years in the tAUS and nBUS. Decadal and multidecadal variations are reported for sea surface temperature and salinity, stratification and subsurface oxygen. Future climate warming is likely associated with a southward shift of the South Atlantic wind system. While the mixing-driven tAUS will most likely be affected by warming and increasing stratification, the nBUS and sBUS will be mostly affected by wind changes with increasing winds in the sBUS and weakening winds in the northern nBUS.

Abbreviations

ABA	Angola-Benguela area
ABFZ	Angola-Benguela Frontal Zone
AC	Angola Current
BC	Benguela Current
BCC	Benguela Coastal Current
BLLCJ	Benguela Low Level Coastal Jet
BOC	Benguela Offshore Current
CMIP6	Coupled Model Intercomparison Project phase 6
ENSO	El Niño-Southern Oscillation
ESACW	Eastern South Atlantic Central Water
EUC	Equatorial Undercurrent
GC	Guinea Current
GCUC	Gabon-Congo Undercurrent
GUC	Guinea Undercurrent
LOW	Low-Oxygen Water
nBUS, sBUS	Northern, southern Benguela Upwelling System
OMZ	Oxygen Minimum Zone
PUC	Poleward Undercurrent
SAA	South Atlantic Anticyclone
SACW	South Atlantic Central Water
SEC, nSEC, cSEC, sSEC	South Equatorial Current and its northern, central, and southern branches
SEJ	Shelf-edge jet
SEUC	South Equatorial Undercurrent

SECC	South Equatorial Countercurrent
SST	Sea Surface Temperature
tAUS	Tropical Angolan Upwelling System

9.1   Introduction

At the eastern boundaries of the tropical and subtropical Atlantic and Pacific oceans, four highly productive ecosystems are located. In the southeastern Atlantic, the Benguela Current Large Marine Ecosystem sustains important fisheries for the three coastal countries Angola, Namibia, and South Africa (Jarre et al. 2015b; Kainge et al. 2020). This region undergoes important climate variability such as extreme warm and cold events off Angola and Namibia, which are termed Benguela Niños and Niñas, respectively (Shannon et al. 1986). They do not only have drastic consequences for the marine ecosystem (Gammelsrød et al. 1998) but also influence the climate over large parts of southern Africa (Reason and Smart 2015; Rouault et al. 2003). Ongoing climate change will affect the eastern boundary regions among others by its effect on the wind field and the resulting wind-driven upwelling, by enhanced warming, increased stratification and ocean deoxygenation (Gruber 2011). Climate predictions for this region using climate models are mostly hampered by long-standing biases in the climate mean-state and variability (Li et al. 2020; Richter 2015; Richter and Tokinaga 2020). Improving predictions of climate and associated impacts on biogeochemistry and ecosystems strongly relies on the representation of the oceanic and coastal upwelling and related processes (Zuidema et al. 2016).

Following Jarre et al. (2015b), the eastern boundary upwelling system of the South Atlantic can be divided into three subsystems: the tropical Angolan upwelling system (tAUS, ~6–17°S), the northern Benguela upwelling system (nBUS, ~17–27°S) and the southern Benguela upwelling system (sBUS, ~27–35°S) that can roughly be associated with the three coastal countries, Angola, Namibia and South Africa, respectively (Fig. 9.1). Typical characteristics of the physical forcing of the marine ecosystems and their temporal variability varies among these subsystems. Southeasterly trade winds prevail in the southeastern Atlantic connecting the subtropical and tropical atmosphere (Fig. 9.1b). The strongest winds are found in the nBUS off the Namibian coast and are associated with the atmospheric Benguela Low Level Coastal Jet (BLLCJ) (Patricola and Chang 2017). The BLLCJ marks the boundary between the Angolan Low and the South Atlantic Anticyclone (SAA). In the tAUS, north of about 17°S, winds are substantially weaker with marginal seasonal variations marked by slightly enhanced southerly winds in austral spring and calm winds in austral winter. The seasonal variations in the position of the SAA with a northwestward shift in austral autumn and a southeastward shift in austral spring result in westerly winds during winter in the sBUS, while southerly winds in the nBUS remain relatively steady throughout the year (Veitch et al. 2009).

The wind-driven ocean circulation is characterized by vigorous zonal currents in the equatorial region and mostly meridional currents along the eastern boundary of the South Atlantic (Fig. 9.1a). Among the most energetic currents is the Equatorial
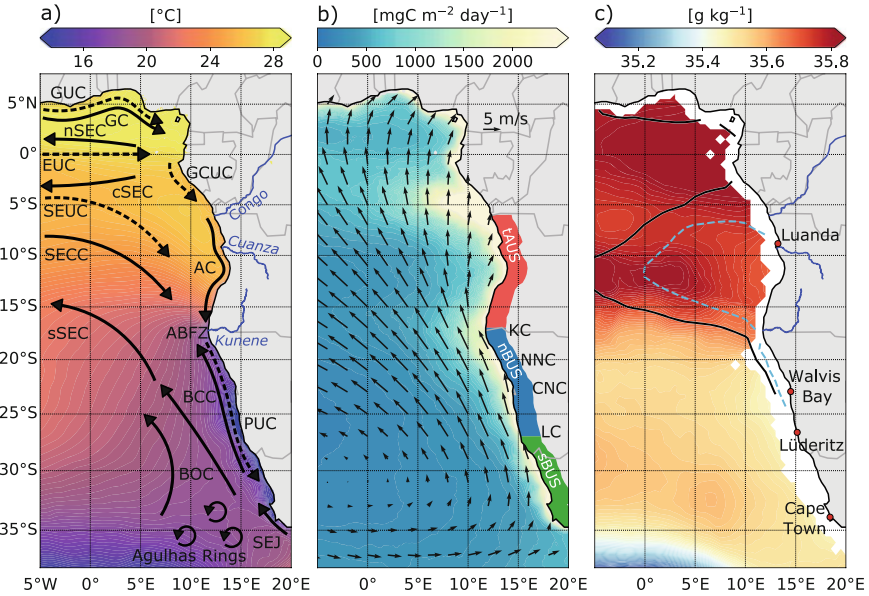
Fig. 9.1 Mean background conditions and circulation schematic for the eastern boundary upwelling system of the South Atlantic. (**a**) Sea surface temperature in the eastern tropical and subtropical South Atlantic obtained from OSTIA-SST with circulation schematic superimposed, (**b**) net primary production as deduced from satellite observations from Ocean Productivity site with surface wind vectors (ASCAT) superimposed and (**c**) absolute salinity on the potential density surface $\sigma_\theta = 26.3$ kg m^{-3} (Argo float data averaged for 2006–2020). Data in (**a**) and (**b**) are averaged for 2002–2019. In (**a**), surface (solid arrows) and thermocline (dashed arrows) current branches shown are the Guinea Undercurrent (GUC), the Guinea Current (GC), the Equatorial Undercurrent (EUC), the northern, central and southern branches of the South Equatorial Current (nSEC, cSEC and sSEC), the South Equatorial Undercurrent (SEUC), the South Equatorial Countercurrent (SECC), the Gabun-Congo Undercurrent (GCUC), the Angola Current (AC), the Poleward Undercurrent (PUC), the Benguela Offshore and Coastal Currents (BOC and BCC), and the shelf-edge jet (SEJ). Also marked in (**a**) is the Angola-Benguela Frontal Zone (ABFZ) at about 17°S and the three rivers Congo, Cuanza and Kunene. In (**b**) the latitude range of the three subregions, the tropical Angolan and the northern and southern Benguela upwelling systems (tAUS, nBUS, sBUS) as well as mean latitudes of the dominant upwelling cells, the Kunene cell, the Northern Namibian cell, the Central Namibian cell and the Lüderitz cell (KC, NNC, CNC, LC) are marked. In (**c**), the 70 μmol kg^{-1} oxygen concentration contours at 130 m depth (light blue dashed line) and at 250 m depth (black line) are included. Oxygen data is from Schmidtko et al. (2017)

Undercurrent (EUC) transporting South Atlantic Central Water (SACW) from the western boundary eastward (Johns et al. 2014). When approaching Africa, most of the water recirculates into the South Equatorial Current (SEC), forming a northern branch (nSEC) slightly north of the equator and a central branch (cSEC) south of the equator (Kolodziejczyk et al. 2014). Along the northern coast of the Gulf of Guinea, the slightly offshore located Guinea Current (GC) and the Guinea Undercurrent (GUC) attached to the continental slope flow toward the eastern boundary (Fig.

9.1a) (Djakouré et al. 2017; Herbert et al. 2016). The equatorward extension of the GC and the GUC, together with the remnants of the EUC, supply the southward Gabon-Congo Undercurrent (GCUC) (Wacongne and Piton 1992), which continues as the Angola Current (AC) in the tAUS (Kopte et al. 2017), and eventually as the Poleward Undercurrent (PUC) through the nBUS into the sBUS (Mohrholz et al. 2008; Nelson 1989). Additional transport of SACW toward the east and the south originating in the near-equatorial belt is carried by the South Equatorial Undercurrent (SEUC) mainly at the thermocline level and by the South Equatorial Countercurrent (SECC) (Siegfried et al. 2019). Along the eastern boundary, the generally southward flowing SACW meets the colder and fresher Eastern SACW (ESACW) flowing northward within the Benguela Current (BC). The confluence of these two currents at about 17°S causes a strong meridional sea surface temperature (SST) gradient that is termed the Angola-Benguela Frontal Zone (ABFZ) (Fig. 9.1). The BC can be described as being composed of an offshore branch (Benguela Offshore Current, BOC) and a coastal branch (Benguela Coastal Current, BCC) (Siegfried et al. 2019). After converging in the ABFZ, the eastern boundary flow turns westward, forming—together with the BOC—the southern branch of the SEC (sSEC) that constitutes the main westward branch of the South Atlantic subtropical gyre.

The surface ocean at the eastern boundary is characterized by the presence of warm and fresh tropical surface water in the northern tAUS, a salinity maximum in the southern tAUS and colder and slightly fresher surface waters south of the ABFZ (Fig. 9.1). South of the ABFZ the surface shows a particular temperature minimum along the coast that is characteristic for the permanent wind-driven coastal upwelling in the nBUS. The sBUS is connected to the Agulhas Current that transports warmer waters from the Indian Ocean around the southern tip of Africa. The two upper-ocean water masses in the region, the SACW and the ESACW, are quite distinct on a specific density surface with SACW being characterized by higher salinities compared to ESACW (Fig. 9.1c). SACW is the water mass of the southern hemisphere subtropical gyre, which is transported by the North Brazil Current toward the equatorial current system and eventually reaches the eastern boundary via the different eastward current branches mentioned above. When arriving at the eastern boundary, it is already low in oxygen with oxygen being further reduced due to high consumption near the highly productive eastern boundary upwelling system. In the area of the ABFZ, it meets the equatorward-flowing oxygen-rich ESACW representing a mixture of SACW and Indian Ocean central water formed in the Cape Basin (Duncombe Rae 2005; Mohrholz et al. 2008). Below the surface layer, the SACW arriving from the north and flowing further poleward within the PUC is thereby continuously mixed with the ESACW and eventually upwells in the northern Benguela (Mohrholz et al. 2008).

The oxygen distribution at the eastern boundary of the South Atlantic is characterized by an open ocean oxygen minimum zone (OMZ) approximately located between the equator and 20°S with a core depth of about 400 m (Karstensen et al. 2008; Monteiro et al. 2008). The OMZ is a result of weak ventilation in a region bounded by the BC and sSEC in the south and the well-ventilated equatorial

region in the north (Brandt et al. 2015). Theoretically, the existence of the OMZ is explained by the Ekman pumping (i.e., the wind stress curl-driven vertical transport out of the oceanic mixed layer into the stratified ocean below) in the area of the SAA resulting in a geostrophic thermocline flow toward the west and the equator thereby forming the shadow zone of the ventilated thermocline (Luyten et al. 1983). Closer to the surface, local oxygen consumption due to high primary production plays a more important role and low-oxygen regions with partly anoxic conditions are found on the shelf as far south as 26°S (Bartholomae and van der Plas 2007) or even in the sBUS in shallow, near-coastal regions (Jarre et al. 2015a).

Although the primary productivity is high along the whole eastern boundary from the Gulf of Guinea to the southern tip of Africa (Fig. 9.1b), the processes relevant for the nutrient supply required to support the primary productivity might vary substantially across the different subregions. While there is high productivity at about 6°S reaching far offshore and driven by the enhanced nutrient supply associated with the river run-off of the Congo (Hopkins et al. 2013; Sena Martins and Stammer 2022), the enhanced near-coastal productivity along the eastern boundary is instead driven by an upward supply of nutrients to the euphotic zone. Physical drivers of the upward nutrient supply are (1) alongshore winds resulting in a near-surface offshore Ekman transport (i.e., the wind-forced horizontal transport perpendicular to the wind direction) supplied by near-coastal upwelling, (2) the cyclonic wind stress curl driving Ekman suction near the coast (i.e., the wind stress curl-driven vertical transport into the oceanic mixed layer out of the stratified ocean below) and (3) upwelling associated with the passage of coastal trapped waves and vertical mixing (Fig. 9.2) (Bordbar et al. 2021; Zeng et al. 2021).

Main topics that will be addressed in this chapter are the mean state and the seasonal cycle of the eastern boundary circulation, upwelling processes, associated biological productivity and low-oxygen regions that are expected to expand under warming climate conditions. We will present main characteristics of the observed interannual to decadal variability, including extreme warm and cold events, decadal temperature and wind changes and evidence of ongoing oxygen changes. Possible future changes will be discussed by using model projections for warming climate scenarios. To capture a comprehensive picture of climate variability and change, a recommendation for the development of the observing system will be provided.

9.2   Eastern Boundary Upwelling System of the South Atlantic

The different physical drivers of the Benguela Current Large Marine Ecosystem that extends from the Congo River mouth to the southern tip of Africa are the basis of three different subsystems: the tAUS, the nBUS and the sBUS. Main differences are (1) warm tropical surface waters in the tAUS compared to cooler subtropical surface waters in the nBUS and sBUS (Fig. 9.3b), (2) strong wind forcing and corresponding wind-driven upwelling resulting in high primary productivity in the nBUS and sBUS compared to the weak wind forcing in the tAUS (Fig. 9.3a and c) and (3) permanent upwelling in the nBUS compared to strong seasonal variability in the tAUS and
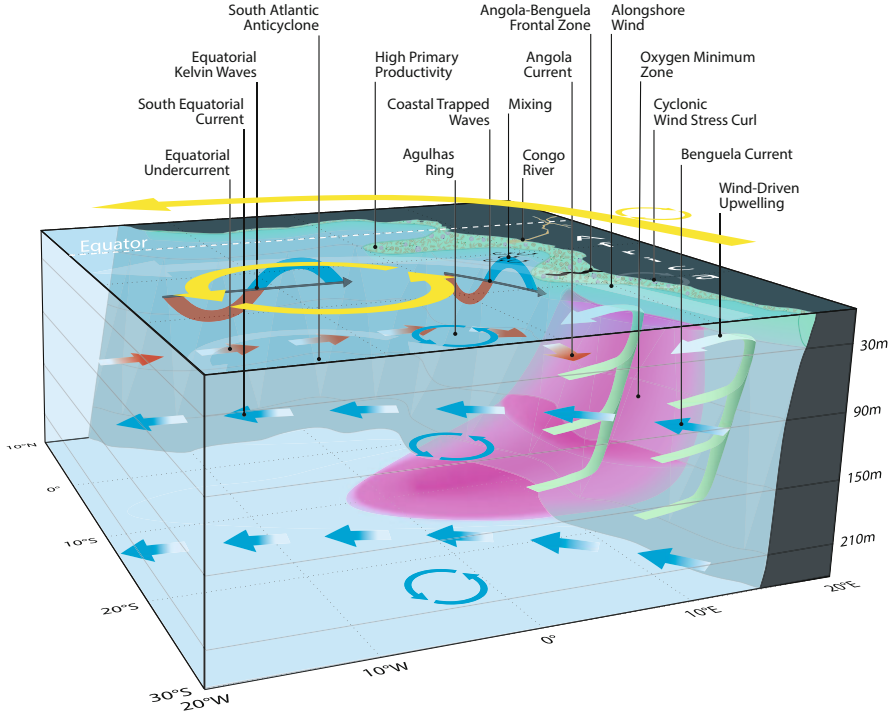
Fig. 9.2 Schematic view of the upper-ocean dynamics and the wind forcing in the southeastern Atlantic. The anticyclonic wind stress curl in the subtropics of the South Atlantic is associated with southerly winds along the African coast. The wind maximum is shifted slightly offshore resulting in a cyclonic wind stress curl in near-coastal areas. Both alongshore winds and cyclonic wind stress curl drive the upwelling in the sBUS and nBUS, which supplies the nutrients for the high primary productivity. In the tAUS, north of the Angola-Benguela Frontal Zone, winds are weak and the upwelling is mostly associated with the propagation of coastal trapped waves mainly forced via equatorial Kelvin waves impinging at the eastern boundary. Mixing during the upwelling wave phases plays the major role in supplying nutrients to the euphotic zone. Further to the north, south of the equator, high primary productivity is associated with nutrient input from the Congo River. Low-oxygen regions that extend far into the open ocean are found mainly north of the Angola-Benguela Frontal Zone and south of the equator. Further to the south, mostly associated with high productivity and enhanced oxygen consumption, low-oxygen regions (partly even anoxic regions) can be found on the shelf in the nBUS and locally in the sBUS

sBUS (Fig. 9.4). Oceanic oxygen conditions reveal the existence of a deep OMZ in the tAUS, extremely low-oxygen conditions on the shelf in the nBUS and only locally low-oxygen conditions in shallow waters on the shelf in the sBUS (Fig. 9.5). The three subsystems are described in the following subsections.
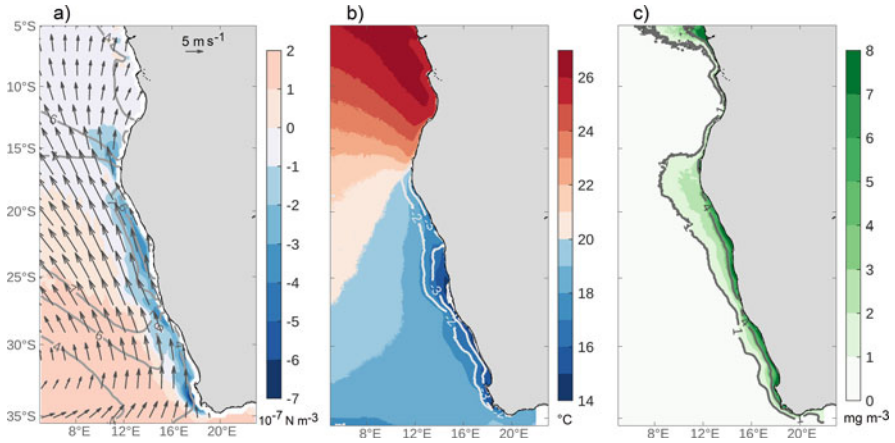
Fig. 9.3 Climate mean-state in the eastern boundary upwelling system of the South Atlantic. (**a**) Surface wind velocity (arrows; m s^{-1}), wind speed (solid grey lines; m s^{-1}) and wind stress curl (color shading; N m^{-3}) computed from ASCAT records over 2008–2020 (Ricciardulli and Wentz 2016). (**b**) SST (color-shading; °C) and SST-based upwelling index calculated as described in Bordbar et al. (2021) (solid white lines; °C) derived from MODIS-Aqua data from 2003 to 2020. (**c**) Chlorophyll-a concentration (color-shading; mg m^{-3}) computed from the MODIS-Aqua product between 2003 and 2020 (NASA Goddard Space Flight Center 2018). Note that solid lines in (**c**) indicate 1.0 and 4.0 mg m^{-3} chlorophyll-a concentration

9.2.1   The Tropical Angolan Upwelling System

The near-coastal area between the Congo River mouths and the ABFZ hosts the tAUS. It is characterized by a tropical stratification with fresh and warm waters at the surface located above saltier waters below. Freshwater input is due to precipitation and the main rivers, the Congo with the river mouth at about 6°S and the Cuanza at about 9°S. Along the coast, a weak southward current, the AC, transports SACW from the equatorial region toward the ABFZ (Tchipalanga et al. 2018). The mean core velocity of the AC at 11°S was found to be only 5–8 cm s^{-1} at a depth of about 50 m superimposed by substantially stronger intraseasonal, seasonal and interannual variability (Kopte et al. 2017). Alongshore winds and near-coastal wind stress curl are generally weak and are not suitable to produce a mean wind-driven upwelling system as it is found further south in the nBUS (Ostrowski et al. 2009; Zeng et al. 2021).

The oxygen distribution off Angola is characterized by the presence of an eastern boundary OMZ that was first described using data from the German Atlantic Meteor Expedition by Wattenberg (1929). It is located between the oxygen-richer regions at the equator and the paths of the BC and sSEC (Fig. 9.1c). The OMZ is a consequence of reduced oxygen supply in the shadow zones of the ventilated thermocline as theoretically predicted by Luyten et al. (1983) in combination with enhanced oxygen consumption due to high primary productivity. Dissolved oxygen concentration in the OMZ off Angola was measured regularly below 35 µmol kg^{-1} with lowest
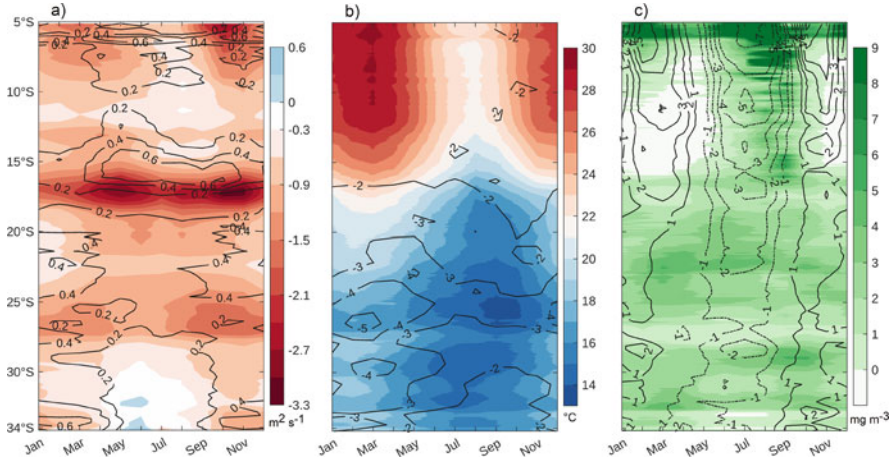
Fig. 9.4 Climatological seasonal cycles in the eastern boundary upwelling system of the South Atlantic. (**a**) Ekman offshore transport (color shading; m^2 s^{-1}) and wind stress curl-driven upwelling velocity (contours; m d^{-1}), (**b**) SST (color shading; °C) and the upwelling index based on SST (contours; °C), and (**c**) chlorophyll-a concentration (color shading; mg m^{-3}) and sea level anomaly (contour; cm). In (**a**) Ekman transport is the zonal transport in the nearest grid point to the coast, whereas the wind stress curl-driven upwelling, SST, SST-based index, chlorophyll-a concentration and sea level anomaly were averaged over a 150 km band along the coast. The reference period for (**a**) and (**b**) is 2008–2020 and 2003–2020, respectively. The climatological monthly mean for chlorophyll-a concentration and sea level anomaly in (**c**) were computed over 2003–2020 and 1993–2018, respectively
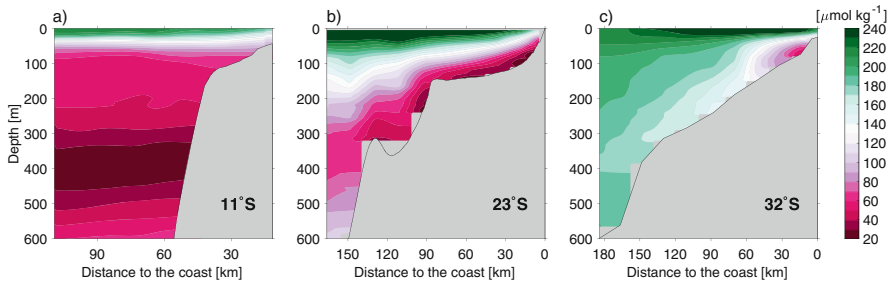

Fig. 9.5 Mean oxygen distribution across the continental slope and shelf. (**a**) Dissolved oxygen concentration along 11°S in the tAUS, (**b**) 23°S in the nBUS and (**c**) 32°S in the sBUS. Mean oxygen values were derived from repeat shipboard hydrographic sections

values close to the eastern boundary at about 400 m depth (Fig. 9.5a). The OMZ off Angola is thus more pronounced than its northern hemisphere counterpart, but substantially more oxygenated than the OMZs at the eastern boundary of the Pacific Ocean (Karstensen et al. 2008).

The seasonal cycle of SST is characterized by low temperatures during austral winter (JAS) and generally warmer waters from November to May (Fig. 9.4b). The

seasonal cycle is mostly controlled by that of the atmospheric fluxes, specifically the solar radiation and the latent heat flux. Upper-ocean warming due to shortwave radiation experiences its annual minimum during austral winter primarily because of a seasonal maximum in solar zenith angle and the expansion of the stratocumulus cloud deck. The seasonal cooling due to the latent heat flux peaks in May which is associated with weak seasonal changes of relative humidity and wind speed (Scannell and McPhaden 2018). Sea surface salinity (SSS) is strongly reduced after maximum rainfall and river discharge of the Congo and Cuanza rivers at the beginning of the year (Sena Martins and Stammer 2022). Low-salinity waters are first observed in January off northern Angola directly south of the Congo River mouth and a few months later further to the south (Lübbecke et al. 2019). During some years the reduction in SSS during late austral summer and autumn can be observed to approach the ABFZ. A secondary minimum in SSS is regularly observed in November and December (Kopte et al. 2017).

The generally weak winds undergo a seasonal cycle with weakest southerly (upwelling-favorable) winds during the main upwelling season from July to September corresponding to a reduced Ekman offshore transport (Fig. 9.4a). Similarly, the wind stress curl-driven upwelling is particularly weak during austral winter north of the ABFZ (Fig. 9.4a). Thus, the winds are suggested not to be responsible for the high primary productivity occurring off Angola during this period (Fig. 9.4c) (Ostrowski et al. 2009; Zeng et al. 2021). The seasonal upwelling and downwelling phases in the tAUS associated with the upward and downward movement of the thermocline (Kopte et al. 2017) are instead predominantly remotely forced from the equatorial Atlantic. Semiannual wind forcing along the equator generates semiannual equatorial Kelvin waves that, when arriving at the eastern boundary, transfer part of their energy into poleward propagating coastal trapped waves. These waves can be observed in sea level anomaly (SLA) data, where elevated sea level indicates a depressed thermocline and vice-a-versa. Maxima in SLA are observed along the eastern boundary off Angola in February and October corresponding to the onset of the main and secondary downwelling seasons, respectively. The months of June and December mark the onset of the main and secondary upwelling seasons, coinciding with the observed minima in SLA during these periods (Fig. 9.4c) (Rouault 2012). The enhanced seasonal cycle of SLA along the eastern boundary could be related to a resonance of the equatorial basin established by eastward and westward propagating equatorial Kelvin and Rossby waves, respectively. At the eastern boundary, this resonance results in an enhancement of the semiannual and annual cycles, however, of different vertical structure (second baroclinic mode for the semiannual cycle compared to a higher baroclinic mode of the annual cycle) (Brandt et al. 2016; Kopte et al. 2018).

The stratification of the upper ocean in the tAUS is related to the vertical movement of the thermocline and further impacted by atmospheric heat and freshwater fluxes and river run-off. Strong upper-ocean stratification is observed during the downwelling seasons (February to April and October, November), while the stratification is weak during July to September (Kopte et al. 2017; Zeng et al. 2021). In the absence of upwelling-favorable winds, vertical mixing might be the main process responsible for the upward transport of nutrients into the euphotic

zone. Zeng et al. (2021) could indeed show by using a tidal model that mixing induced by internal tides generated at the continental slope and propagating toward the coast contribute to near-coastal mixing (i.e., water shallower than 50 m) and associated local reduction of SST. Higher primary productivity during the main upwelling season could be explained as a result of weaker stratification: while the tidal energy available for mixing is almost constant throughout the year, the reduced stratification during austral winter allows stronger mixing and results in enhanced surface cooling and upward nutrient supply near the coast.

Superimposed on the seasonal cycle are intraseasonal or subseasonal fluctuations most prominently visible in SLA data and subsurface moored velocity records (Kopte et al. 2017; Polo et al. 2008). They are associated with coastal trapped waves either locally generated by local wind fluctuation or remotely generated along the equator or even further upstream in the tropical North Atlantic (Illig et al. 2018; Imbol Koungue and Brandt 2021). Contrary to the eastern boundary in the South Pacific, where such waves can coherently be observed in SLA data from the equator to about 27°S, in the South Atlantic the signal fades out already at 12°S. The difference could be explained by the higher baroclinic modes in the Atlantic compared to the Pacific, where the first baroclinic mode dominates, resulting in a stronger dissipation of wave energy along its path in the Atlantic (Illig et al. 2018). Intraseasonal coastal trapped waves off Angola show particular spectral peaks at about 90 and 120 days. These waves are mostly associated with remote equatorial forcing either by zonal wind forcing in the eastern equatorial Atlantic (90-day waves) or by the establishment of a resonant equatorial basin mode (120-day waves), respectively. The superposition of the intraseasonal waves with seasonal or interannual waves was found to be able to enhance or reduce the seasonal cycle as well as to impact Benguela Niños and Niñas (Imbol Koungue and Brandt 2021).

9.2.2   The Northern Benguela Upwelling System

The nBUS stretches between the ABFZ in the north and the Lüderitz upwelling cell in the south and is the transition zone between two source water masses, tropical SACW and subtropical ESACW (Junker et al. 2017; Mohrholz et al. 2008). The SACW, that dominates the region north of about 17°S, is warmer and more saline than the ESACW (Fig. 9.1c). It carries nutrients and is oxygen depleted. In contrast, the ESACW is well oxygenated. Over the nBUS, the fraction of SACW is decreasing poleward between unity near the ABFZ and almost zero near the Lüderitz upwelling cell. Hence, temperature and salinity but also the macronutrient and oxygen concentrations vary throughout the nBUS.

Figure 9.6, which represents a long-term average (2002 to 2016) produced from output of an ocean circulation model (Bordbar et al. 2021; Siegfried et al. 2019), shows the general circulation pattern guiding SACW and ESACW toward the nBUS. The simulated flowlines shown here follow the isopycnal $\sigma_\theta = 26.3$ kg m^{-3}. Since potential density of a water mass is conserved below the surface layer, flowlines on a certain density level depict the spreading of the water mass with this specific
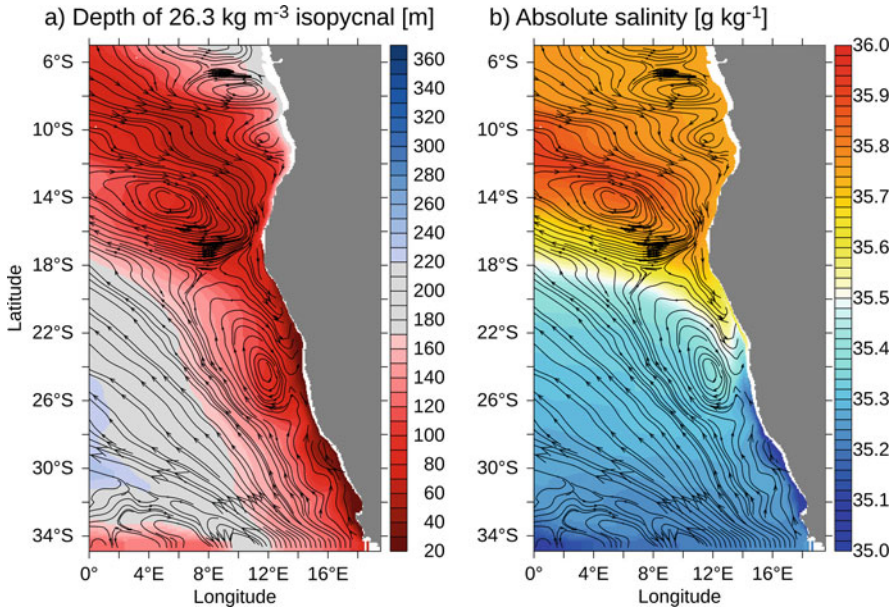
Fig. 9.6 Circulation and characteristics of the core water mass that upwells along the Southwest African coast. The water mass is defined by the potential density $\sigma_\theta = 26.3 \text{ kg m}^{-3}$. (**a**) Depth of the isopycnal $\sigma_\theta = 26.3 \text{ kg m}^{-3}$ overlaid with flowlines. (**b**) Salinity on the isopycnal $\sigma_\theta = 26.3 \text{ kg m}^{-3}$ overlaid with flowlines. The isopycnal $\sigma_\theta = 26.3 \text{ kg m}^{-3}$ outcrops in the nBUS and the sBUS with water upwelling into the surface layer. The upwelled water originates from different source regions. The salinity distribution reveals the role of the nBUS as a mixing hotspot between water of tropical and subtropical origin. Results are derived from an ocean circulation model

density. Figure 9.6a shows the depth of the $\sigma_\theta = 26.3 \text{ kg m}^{-3}$ isopycnal. Water with this density outcrops and is upwelled in the nBUS and the sBUS, indicating it as a core water mass of the whole BUS. Also, in the north at around 8°E, 14°S, the $\sigma_\theta = 26.3 \text{ kg m}^{-3}$ isopycnal is elevated and associated with a cyclonic flow pattern. Some flowlines are continuing from the northern rim of this pattern into the nBUS suggesting the transport of warm and high-saline SACW from the tropical Atlantic into the nBUS (Lass and Mohrholz 2008). Similarly, flowlines starting in the south, e.g., at 35°S near the eastern boundary (Fig. 9.6), ending up in the nBUS revealing the northward transport of cold and fresh ESACW.

The long-term averaged flow is essentially in Sverdrup balance (Mohrholz et al. 2008; Siegfried et al. 2019; Small et al. 2015) by which the wind stress curl (Fig. 9.3a) determines the vertically integrated circulation. The simulated circulation shown in Fig. 9.6 is more general and also considers baroclinic details. However, its large-scale flow features can be understood from the Sverdrup balance: The northwestward flow off Namibia and South Africa (cf. BOC in Fig. 9.1) is related to the large-scale anticyclonic wind stress curl (Fig. 9.3a). In turn, the broad band of the southeastward directed flow off Angola corresponds to the area with weak but

extended cyclonic wind stress curl. The Sverdrup balance also explains the sudden westward turn of the flow at about 16°S as related to a permanently present patch of strongly enhanced cyclonic wind stress curl in the Kunene upwelling cell (Fig. 9.3a). South of the ABFZ the numerical model results show a strong poleward flow that leaves the shelf with another westward turn near the Lüderitz upwelling cell at about 26°S.

The almost alongshore wind drives the coastal upwelling in the entire nBUS (Bordbar et al. 2021; Junker et al. 2015; Lass and Mohrholz 2008). The upwelled water is SACW and ESACW originating from just below the surface mixed layer down to approximately 200 m depth (Siegfried et al. 2019). It forms a narrow coastal band of nutrient-enriched surface water with relatively low temperature and enhanced chlorophyll-a concentration, which is visible in satellite-derived data (Fig. 9.3). In the nBUS the SST contrast between coast and open ocean locally amounts to more than 3°C (Fig. 9.3b) and is particularly large in the area between Walvis Bay and Lüderitz (Fig. 9.1). Here, features like fronts and filaments are observed that govern the exchange of heat and matter between the coastal and the open ocean (Bettencourt et al. 2012; Hösen et al. 2016; Mohrholz et al. 2008; Muller et al. 2013; Veitch and Penven 2017). Strength and seaward extension of upwelling in the nBUS vary along the coast and features several upwelling cells with characteristically low coastal SST (Bordbar et al. 2021; Chen et al. 2012; Shannon 1985). The most prominent cells are the Kunene cell at 17°S and the Lüderitz cell at 27°S (Fig. 9.4). Other upwelling cells are the Northern Namibian cell at 20°S and the Central Namibian or Walvis Bay cell at 23°S. The typical "coastal drop" of the alongshore wind off Namibia, i.e., coastal winds are weaker than the winds offshore, implies a cyclonic wind stress curl. The associated Ekman suction causes upwelling and plays an important role in the offshore region of the entire BUS (Figs. 9.3a and 9.4a) (Fennel 1999; Fennel et al. 2012). In general, the spatial pattern of the cyclonic wind stress curl narrows poleward, which matches the pattern of chlorophyll-a concentration fairly well (Fig. 9.3) (Bordbar et al. 2021; Fennel 1999). The Ekman suction shows seasonal maxima and minima appearing during different times of the year in the different cells. In the Kunene cell it is enhanced during March–October, whereas it peaks between September and April in the Walvis Bay cell at 23°S (Fig. 9.4a). The SST-based upwelling index is intensified between March and June everywhere across the nBUS (Fig. 9.4b), which follows the pattern of neither the coastal upwelling nor the Ekman suction.

The wind-driven upwelling is accompanied by swift geostrophic alongshore currents composed of the equatorward coastal jet at the surface and the PUC, an offshore countercurrent at subsurface. The structure and the relative strengths of the different eastern boundary current branches are governed by the separation of the alongshore wind maximum from the coast and the magnitude of the associated onshore wind stress curl (Fennel 1999; Fennel et al. 2012). The coastal jet amounts up to about 0.4 m s^{-1} near the ABFZ at about 17°S with velocities decreasing southward (Junker et al. 2019). In large-scale circulation maps it is often marked as the coastal branch of the Benguela Current (Fig. 9.1a). Associated with the reduced wind north of the Kunene cell, the coastal jet almost disappears there. Here, the
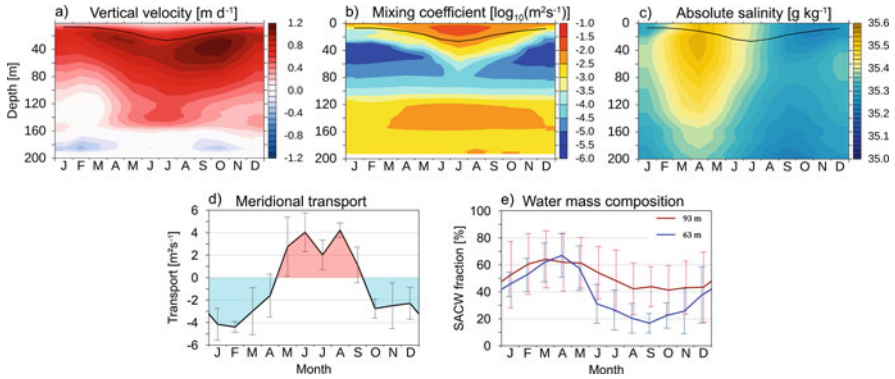
Fig. 9.7 The Walvis Bay upwelling cell at 23°S. Climatological seasonal cycles off Walvis Bay of (**a**) vertical velocity, (**b**) vertical mixing coefficient, (**c**) salinity. The quantities are the areal average over a 1° × 1° rectangle around 14°E, 23°S. The black line indicates the mixed layer depth. The monthly climatology (2002–2016) is derived from the results of an ocean circulation model forced by observed momentum, heat and mass fluxes (Bordbar et al. 2021; Siegfried et al. 2019). Climatological seasonal cycles of (**d**) meridional transport and (**e**) water mass composition (SACW vs. ESACW) at 63 m (red line) and 93 m (blue line) based on data from a mooring operated from 2003 to 2016 at 14°E, 23°S (Junker et al. 2017). Note that positive (negative) values in (**d**) indicate equatorward (poleward) transport. Whiskers represent the monthly climatological standard deviation

AC arriving from the north merges with PUC and continues southward through the ABFZ into the nBUS (Mohrholz et al. 2008).

In the following, we will describe the physical processes within the Walvis Bay upwelling cell at 23°S based on results from an ocean model simulation (Bordbar et al. 2021; Siegfried et al. 2019) and measurements taken by a long-term mooring on the Namibian shelf (14°E, 23°S) at a water depth of about 130 m (Junker et al. 2017). The vertical velocity (Fig. 9.7a) is primarily driven by the alongshore wind and peaks near the mixed layer depth (Fennel et al. 2012). Its seasonal cycle follows that of the alongshore wind with maxima in April and October. The mixed layer deepens from June to September concurrent with the lowest seasonal SST (Fig. 9.4b). Vertical mixing (Fig. 9.7b) forces entrainment of subsurface water into the surface mixed layer and is controlled by both, the seasonal cycle of the wind and the net surface heat flux. The maximum vertical mixing occurs in July and is concurrent with surface cooling (Fig. 9.4b) and deepening of the mixed layer. The seasonal variation of the salinity off Walvis Bay is visible over the entire upper 200 m depth (Fig. 9.7c). Salinity exhibits a seasonal maximum in April and a minimum in September corresponding to a dominance of SACW and ESACW, respectively. The meridional transport on the shelf as observed at the mooring position (Fig. 9.7d) (Junker et al. 2017; Mohrholz et al. 2008) shows a seasonal flow reversal that can be attributed to the seasonal cycle of the local wind stress curl (Junker et al. 2015). The observed flow is directed poleward from October–April and directed equatorward from March–September, which leads to the alternating influences of SACW and

ESACW on the Namibian shelf visible in the water mass fractions as obtained from moored hydrographic measurements (Fig. 9.7e). Mohrholz et al. (2008) showed that this alternation regulates the oxygen concentration on the Namibian shelf as well. Local oxygen consumption further modifies the oxygen conditions on the shelf and shapes the very specific ecosystem (Schmidt and Eggert 2016).

9.2.3   The Southern Benguela Upwelling System

The northern and southern Benguela upwelling systems are separated by the perennial Lüderitz upwelling cell, where the continental shelf also narrows abruptly toward the north. The sBUS extends southward from the Lüderitz cell along the entire west coast of South Africa and eastward to Cape Agulhas along the south coast (Boyd and Nelson 1998). Whereas the large-scale, depth integrated flow regime of the nBUS, from the ABFZ to Lüderitz, is driven by the alongshore winds and the wind stress curl, the large-scale dynamics of the sBUS is dominated by nonlinearities via turbulence associated with the shedding of Agulhas Rings, eddies and filaments at the Agulhas retroflection south of the African continent (Veitch et al. 2010). This intense offshore turbulence within the Cape Basin is unique among eastern boundary upwelling systems and presents itself as a distinct juxtaposition to the relatively quiescent shelf region of the sBUS (Veitch et al. 2010). Intense submesoscale variability in the Cape Basin leads to extreme vertical motions that have been shown to reduce productivity in coastal upwelling regions (Gruber et al. 2011) as well as in the offshore domain of the sBUS (Rossi et al. 2008).

The transition between the relatively quiescent shelf and the turbulent offshore region is marked by an intensified shelf-edge jet (SEJ) (Fig. 9.1a). It arises from the geostrophic adjustment of the particularly intense temperature front between the strongly seasonal cold upwelling regime at the coast and offshore waters that are warmed and modulated by highly variable influx of Agulhas waters (Veitch et al. 2018). This jet not only has an important role in transporting fish eggs and larvae from their spawning ground on the Agulhas Bank to their nursery area in St Helena Bay (Hutchings et al. 2009), it also limits cross-shelf exchanges (Barange and Pillar 1992; Pitcher and Nelson 2006). Despite seasonal and higher frequency modulations, the jet is a permanent feature (Nelson and Hutchings 1983) that tends to be situated over the 200–500 m isobaths and has been described as a convergent north-west oriented system on the western Agulhas Bank that funnels into the west coast (Shannon and Nelson 1996), bifurcating at Cape Columbine (32°50′S) where its inshore section veers into St Helena Bay (Lamont et al. 2015).

Satellite imagery (Demarcq et al. 2007; Lutjeharms and Stockton 1987) and model studies (Veitch and Penven 2017) have revealed that upwelling filaments in the southern Benguela do not extend as far offshore as their northern Benguela counterparts. The mean position of the upwelling front is approximately coincident with the location of the shelf-edge (Shannon 1985) and is commensurate with the frontal system that drives the intense SEJ. The limited offshore extent of upwelling filaments is therefore related both to the turbulent influx of warm Agulhas waters

beyond the shelf-edge as well as to the SEJ that serves to inhibit their offshore expansion. While this frontal system helps to maintain the retentive nature of the southern Benguela shelf, it also contributes to the generation of cyclonic eddies that have been observed to form throughout the year in the vicinity of the upwelling front along the 200 m isobath (Lutjeharms and Stockton 1987) and to migrate predominantly in a west-southwestward direction (Hall and Lutjeharms 2011). The modeling results of Rubio et al. (2009) confirmed their generation at the upwelling front followed by their offshore migration, but also quantified the huge volume of water they carry, that could potentially be highly productive coastal waters transporting fish eggs and larvae from the Agulhas Bank to St Helena Bay as well (Hutchings et al. 1998).

Upwelling is strongly seasonal in the sBUS, being strongest during austral spring and summer months (Fig. 9.4a) and modulated with a period of 5–6 days due to the passage of cyclones and continental lows (Nelson and Hutchings 1983). Discrete upwelling cells are located in regions of enhanced wind stress curl and primarily where there are changes in coastline orientation (Lamont et al. 2018; Shannon and Nelson 1996). The two southernmost cells on the west coast, Cape Columbine and Cape Peninsula, are associated with a narrowing of the southern Benguela shelf and the only two prominent embayments of the Benguela system, namely St. Helena Bay and Table Bay. During active upwelling periods a cold plume develops at the distinct promontory of Cape Columbine (Taunton-Clark 1985), while a cyclonic eddy develops in its lee (Penven et al. 2000). These features produce a dynamic boundary between the nearshore and offshore regimes and create a highly retentive region within St. Helena Bay that is crucial for primary production, fish recruitment, but also has implications for low-oxygen water (LOW) on the southern Benguela shelf (Fig. 9.5c).

Aside from the shelf-edge frontal system, the existence of multiple fronts on the broad southern Benguela shelf was conceptualized by Barange and Pillar (1992) and observed by Lamont et al. (2015) to develop and merge in accordance with upwelling-favorable wind conditions. The proposed mechanism of Andrews and Hutchings (1980) that upon reaching a front, offshore advecting particles follow isopycnals and are subducted has been identified as crucial for nutrient-trapping and oxygen dynamics on the southern Benguela shelf (Flynn et al. 2020). This mechanism arises from secondary, ageostrophic circulations associated with frontogenesis and include upward (downward) velocities on the warm (cold) side of fronts (Capet et al. 2008).

The boundaries of the sBUS are dominated by well-ventilated ESACW. The varying presence of southern Benguela LOW is therefore limited to nearshore regions, developing in response to local dynamics (upwelling, retention, stratification and advection) and biogeochemical processes that are strongly dependent on seasonal wind fluctuations (Monteiro and van der Plas 2006). The formation of LOW has been observed throughout the sBUS (Jarre et al. 2015a), but occurs less frequently off the Namaqua shelf than within the St Helena Bay region where hypoxia persists throughout the year in the bottom waters (Fig. 9.5c), suggesting a permanent reservoir of LOW (Lamont et al. 2015). The formation of these low-

oxygen bottom waters is driven by the decay of large phytoplankton blooms in the inner and mid-shelf regions during the upwelling season when retention and stratification is high (Pitcher and Probyn 2017). While wind mixing during winter months causes reoxygenation of the entire water column at nearshore stations, it is unable to erode the LOW reservoir at the bottom at depths greater than 50 m (Lamont et al. 2015). By the beginning of the upwelling season, in early austral spring, the shelf bottom waters are most oxygenated due to the on-shelf entrainment of the well-ventilated ESACW. For the duration of the upwelling season, the bottom oxygen concentrations within St Helena Bay progressively decrease due to continual draw-down of decaying organic matter. Flynn et al. (2020) demonstrated that nutrients available to be upwelled are augmented by regenerated nutrients from the previous summer and early winter that are trapped on the shelf by dynamics associated with the frontal system. This gives rise to enhanced primary production, decay and oxygen consumption. During periods of upwelling-favorable winds, the bottom pool of LOW is advected shoreward, priming the conditions for episodic anoxic events in St Helena Bay that occur toward the end of the upwelling season in the shallower nearshore environments, where high biomass dinoflagellate blooms (or "red-tides") are retained due to persistent downwelling or to the relaxation of upwelling-favorable winds. Their decay causes extreme oxygen consumption and oxygen depletion throughout the water column, leading to rock lobster walk-outs (Cockcroft 2001) as well as to major fish mortalities (Matthews and Pitcher 1996). New high temporal resolution dissolved oxygen measurements between February 2019 and October 2020, off Hondeklip Bay along the Namaqua shelf, revealed minimum oxygen concentrations during austral winter at a location offshore of the upwelling front suggesting the importance of lateral fluxes for the oxygen seasonality. This oxygen seasonality appears to be driven by the breakdown of the upwelling front during winter followed by periods of enhanced lateral mixing, which allows offshore advection of oxygen-depleted water from the nearshore environment (Rixen et al. 2021).

9.3   Interannual Variability

Around the ABFZ, SST varies from year to year with extreme warm and cold events occurring irregularly every few years. These events have been termed Benguela Niños and Niñas, respectively, to highlight their similarity to the Pacific El Niño phenomenon (Shannon et al. 1986). During these events, SST in the Angola-Benguela area (ABA, 8°E-coast; 10–20°S) can exceed the climatological value by more than 2°C (Fig. 9.8).

Both warm and cold events typically start with an SST anomaly off the Angolan coast in austral fall, which then spreads into the eastern equatorial Atlantic in the following months (Fig. 9.9). Since they have been first described in the 1980s, a number of different processes that contribute to the generation of these events have been determined. They can be broadly classified into remote and local forcing mechanisms (Richter et al. 2010). Remote forcing from the equatorial Atlantic
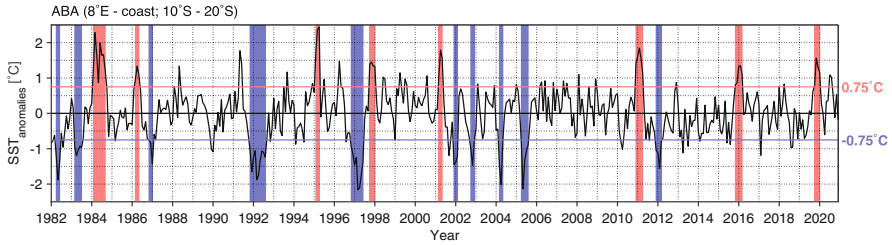
ABA (8˚E - coast; 10˚S - 20˚S)

Fig. 9.8 Monthly detrended interannual SST anomalies (NOAA OISST) averaged in the Angola-Benguela Area (ABA, 8°E-coast; 10–20°S) from January 1982 to December 2020. The red and blue rectangles highlight the extreme warm and cold events in the region, respectively. The horizontal red and blue lines show the standard deviation of the interannual SST anomalies in the ABA. The criterion for an extreme event is defined by an SST anomaly exceeding the threshold of ±1 standard deviation for at least three consecutive months
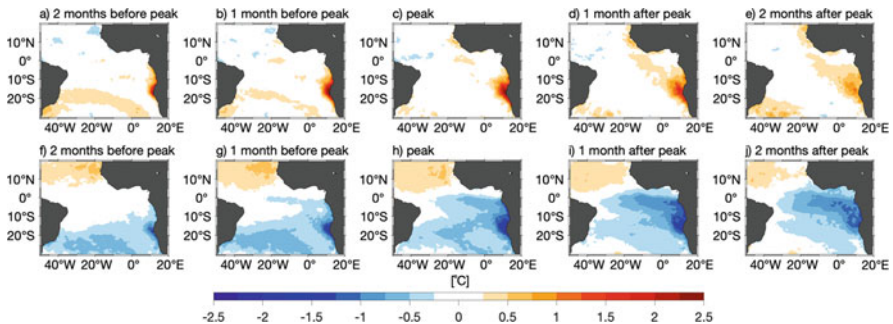
Fig. 9.9 Temporal evolution of Benguela Niños and Niñas. Composite maps of monthly detrended SST anomalies derived from observations (NOAA OISST) and computed from four extreme warm events (1984; 1986; 1995 and 2001) for (**a**) 2 months before the peak, (**b**) 1 month before the peak, (**c**) peak, (**d**) 1 month after peak, (**e**) 2 months after the peak. Bottom panels (**f**–**j**) show the same as (**a**–**e**) but computed from six extreme cold events (1982, 1983, 1992, 1997, 2004 and 2005). Note that we included only extreme events that occurred during the period 1982–2020 and peaked between March and May

happens via the propagation of equatorial and coastal trapped waves. Variations of the zonal wind stress in the western equatorial Atlantic excite equatorial Kelvin waves that propagate eastward along the equatorial waveguide. Once they reach the eastern boundary, part of their energy is transmitted poleward along the African coast as coastal trapped waves. These waves are associated with a deflection of the thermocline that is linked to subsurface and subsequently surface temperature anomalies. A weakening (strengthening) of the easterly trade winds in the western to central equatorial Atlantic excites a downwelling (upwelling) Kelvin wave that is associated with a warm (cold) subsurface temperature anomaly and a strengthening (weakening) of the poleward flow of tropical warm waters, leading to a positive (negative) SST anomaly in the ABA. Many studies have shown the importance of this remote forcing mechanism, both for observed individual events (Florenchie et

al. 2003; Rouault et al. 2018) and as a dominant mechanism in generating SST anomalies off Angola in ocean model simulations (Bachèlery et al. 2016, 2020; Florenchie et al. 2004; Imbol Koungue et al. 2017; Lübbecke et al. 2010). The impact of interannual coastal trapped waves on near-coastal temperatures is found to be strongest in the tAUS and northern nBUS. Based on model simulations, Bachèlery et al. (2020) showed that they are dominantly associated with the second and third coastal trapped wave modes. Coastal trapped waves of the less-dissipative first mode can be traced further south eventually reaching the sBUS, but their impact on near-coastal temperatures is weak.

In addition to the remote forcing, local processes can cause SST anomalies and lead to the generation of Benguela Niño and Niña events (Lübbecke et al. 2019; Polo et al. 2008; Richter et al. 2010). Variations in the local winds result in changes in the wind-driven upwelling of cold subsurface waters, anomalies in the latent heat flux from the ocean to the atmosphere and modulations of the meridional currents. Anomalous freshwater input from precipitation and river run-off might additionally impact SSTs via changes in stratification and the creation of barrier layers that inhibit the upward mixing of cold subsurface waters (Lübbecke et al. 2019). Illig et al. (2020) suggested that local wind forcing is crucial to explain the timing and spatial evolution of Benguela Niños and the subsequent warming in the eastern equatorial Atlantic. Moreover, Hu and Huang (2007) showed using reanalysis data that locally forced warming over the Angola-Benguela upwelling region is likely to generate westerly wind anomalies along the equatorial Atlantic one to two months later. An example of such a connection is the occurrence of the 2019 Benguela Niño (Fig. 9.8) recently studied by Imbol Koungue et al. (2021). This extreme warm event that developed along the coasts of Angola and Namibia between October 2019 and January 2020, was found to be forced by a combination of local and remote forcing with local forcing leading the remote forcing by one month. Remote and local forcing generally can be connected via changes of the SAA (Illig et al. 2020; Imbol Koungue et al. 2019; Lübbecke et al. 2010; Richter et al. 2010).

Benguela Niños and Niñas can have large impacts on the marine ecosystem as well as on the precipitation over Southwest Africa. The extreme warm event of 1995 has been associated with observed mortalities in sardine, horse mackerel and kob (Gammelsrød et al. 1998) as well as a southward shift of the sardine population (Boyer and Hampton 2001). Benguela Niño events are linked to above average rainfall over western Angola and Namibia via enhanced evaporation and moisture flux (Reason and Smart 2015; Rouault et al. 2003) while Benguela Niña events are associated with reduced precipitation along the Angolan coast (Koseki and Imbol Koungue 2021). For the benefits of the southern African countries and the coastal communities, it is thus desirable to predict such warm and cold events. A promising approach toward the prediction of SST anomalies off Angola and Namibia is based on the time it takes the equatorial and coastal waves to cross the basin and propagate poleward along the coast. Imbol Koungue et al. (2017) combined data from real time PIRATA buoys, altimetry and outputs from an ocean linear model to define an index of equatorial Kelvin wave activity. In agreement with the remote forcing mechanism

described above, they found a high correlation for a second-mode equatorial Kelvin wave leading SST anomalies in the ABA by one month.

The sBUS varies primarily due to fluctuations associated with the seasonal shift of the SAA (Shannon and Nelson 1996). Interannual fluctuations in the sBUS, in terms of both upwelling strength and related LOW variability (Johnson and Nelson 1999; Monteiro et al. 2006), are strongly tied to variations in the SAA, which are related to both the phase of the Southern Annular Mode and El Niño-Southern Oscillation (ENSO) (Sun et al. 2019). For instance, Dufois and Rouault (2012) and Rouault et al. (2010) demonstrated that Pacific El Niño events tend to be associated with a northward shift of the SAA and a concomitant reduction of upwelling-favorable winds and enhanced coastal SSTs in the sBUS, with the opposite occurring during Pacific La Niña events. While confirming the influence of ENSO on the position of the SAA, Sun et al. (2019) found, however, no clear relationship between ENSO and the upwelling strength in the sBUS, especially for austral winter.

Located southwest of South Africa, the Agulhas retroflection is an important region of interbasin exchange of heat, salt and energy (Beal et al. 2011) and can also have a direct influence on the nutrient availability and biological responses observed on the adjacent shelf ecosystems (Roy et al. 2007; Roy et al. 2001). Interannual fluctuations of Agulhas leakage therefore have important implications for the sBUS. Using an improved method to identify the location of the core and edges of the Agulhas Current, a recent study by Russo et al. (2021) examined the variability of the Agulhas retroflection between 1993 and 2019. The Agulhas retroflection was located generally between 40.5–38.4°S and 15.0–20.0°E. Although seasonal variations were not statistically significant, the Agulhas retroflection extended further west during summer than in winter. During the 1993–2019 period, a total of seven events with Agulhas retroflections occurring further eastward were identified, with five events (1999, 2000–2001, 2008, 2013, 2019) being classified as early retroflections (east of 22.5°E), and two events (2014 and 2018) associated with the shedding of large Agulhas Rings. Their study described that early retroflection events during the first half of the 1993–2019 period tended to be more extreme but less frequent, while the latter part of study period showed less extreme but more frequent events (Russo et al. 2021). Changes in the mean position of the Agulhas retroflection, as well as the frequency and length of early retroflection events, can substantially impact the influx of Agulhas Current waters. This likely influences the stability and maintenance of the SEJ responsible for transport of fish eggs and larvae from the Agulhas Bank to the west coast of South Africa (Veitch et al. 2018).

9.4   Decadal Variations and Multidecadal Trends

Compared to the global average, the southeastern tropical Atlantic experienced moderate sea surface warming during the last 40 years (Bulgin et al. 2020). For the Southwest African coast, Sweijd and Smit (2020) reported the strongest warming trend near the ABFZ of more than 0.4°C decade^{-1} from 1981 to 2019. Warming
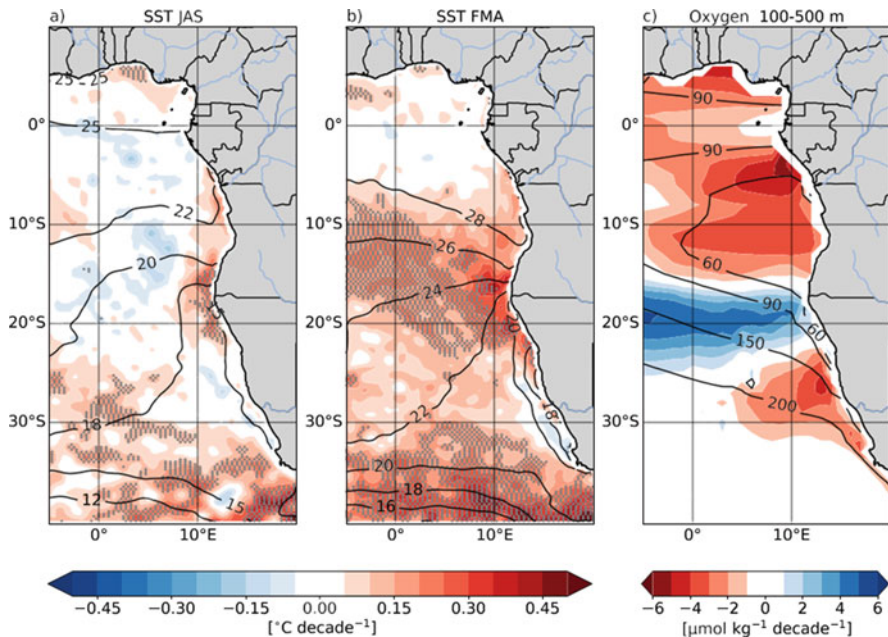
Fig. 9.10 Observed decadal trends in SST and oxygen. SST trends during (**a**) austral winter and (**b**) late austral summer evaluated between 1982 and 2017 using ERA5 reanalysis data (Hersbach et al. 2020). Black contours indicate seasonal mean SST. Grey dots indicate that the linear regressions are significant at the 95% level according to the Student's t-test. (**c**) Dissolved oxygen trend in 100–500 m (μmol kg^{-1} decade^{-1}) for the period 1960–2010. Black contours indicate mean 100–500 m oxygen concentration. Oxygen data is from Schmidtko et al. (2017)

was particularly enhanced in the tAUS and northern nBUS in comparison to the southern nBUS and the sBUS partly even showing cooling trends (Fig. 9.10). Seasonally warming patterns differ substantially with strongest warming during the satellite period observed during late austral summer with more than 0.3°C decade^{-1} (Fig. 9.10b). Vizy and Cook (2016), using high-resolution observations and reanalysis datasets over the period 1982–2013, showed from the analysis of the ocean surface heat balance that the austral summer SST warming trend along the Angolan/Namibian coast is associated with an increase in net surface heat flux. In addition, they showed a decrease in coastal upwelling due to atmospheric circulation changes related to a poleward shift of the SAA and an intensification of the Southwest African thermal low. The observed warming that varied substantially among different SST datasets was found to be associated with a slight southward shift of the ABFZ only (Prigent et al. 2020a; Vizy et al. 2018). However, only weak changes in the latitude of the front are expected as the position is largely determined by the shoreline orientation, bathymetry and associated wind stress (Shannon et al. 1987).

Upper-ocean decadal changes are well-detectable using data from the Argo observation program. Since 2000 the oceans have been filled with Argo floats continuously measuring temperature and salinity from the surface down to 2000 m of the water column within 10-day cycles (Desbruyères et al. 2017; Roemmich et al. 2015). From Argo observations, Roch et al. (2021) suggested that the southeastern Atlantic around the ABFZ is shifting from subtropical to tropical upper-ocean conditions. In this region, the vertical stratification maximum of the thermocline/pycnocline is located only slightly below the mixed layer. Hence, upper-ocean stratification changes can be assumed to be closely linked to mixed layer changes. The trend pattern of the vertical stratification maximum in the southeastern Atlantic that was derived following Roch et al. (2021), reveals a stratification increase of up to 30% decade^{-1} within 7–25°S for the time period of 2006–2020 (Fig. 9.11a). This area is located around the ABFZ. North of this region, which is actually the area with highest stratification values in the mean field, the stratification is decreasing. South of 30°S stratification changes are rather weak. The mixed layer depth shows a strong shoaling trend of around 8 m decade^{-1} within 5°E-coast, 2–18°S during the 2006–2020 period (Fig. 9.11b). This overlaps regionally with the area of the largest stratification increase. Clearly, the shoaling trend of the mixed layer cannot continue in the long-term as the mixed layer thickness has to reach a lower limit. North and south of this region the mixed layer is deepening. Within 30–40°S and west of the 0°-meridian, the deepening is largest with almost 10 m decade^{-1}.

The pronounced stratification enhancement in the area around the ABFZ is associated with a warming and freshening of the mixed layer (up to 2°C decade^{-1} and around 0.3 g kg^{-1} decade^{-1}, respectively, Fig. 9.11c and d). North and south of this region the mixed layer temperature depicts a cooling trend (Fig. 9.11c). However, along the coast from 30°S to Cape of Good Hope, a relatively weak warming trend (up to 0.5°C decade^{-1}) can be observed. In contrast, the freshening of the mixed layer can be found all the way south to 40°S. Yet, east of the 35.8 g kg^{-1} isohaline from the mean field, no trend is found (Fig. 9.11d).

To conclude, the observed enhancement of stratification around the ABFZ during the Argo observation period (2006–2020) together with the warming, freshening and shoaling of the mixed layer resulted in a southward expansion of background conditions associated with tropical upwelling systems (Roch et al. 2021). Besides in the equatorial region, the decrease in stratification can be associated with a cooling and salinification of the mixed layer. In contrast, off the coast of South Africa and southern Namibia weak trends can be observed including a slight warming and a deepening of the mixed layer.

Long-term changes have also been observed in the occurrence of Benguela Niño and Niña events. Prigent et al. (2020a) reported, relative to the period 1982–1999, an about 30% reduction of the March–April–May interannual SST variability around the ABFZ during 2000–2017 (Fig. 9.12). The weakened interannual ABA SST variability goes along with a reduced influence of the remote forcing by equatorial wind stress variability (cf. Sect. 9.3). Indeed, the lower zonal wind stress variability in the western equatorial Atlantic reported by Prigent et al. (2020b) tends to reduce
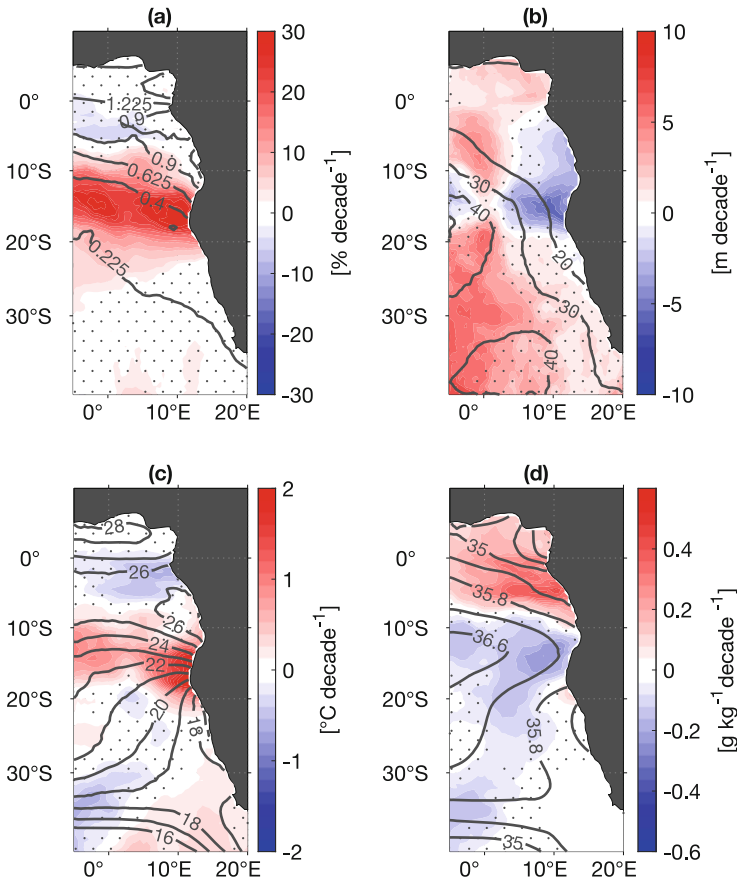
Fig. 9.11 Observed decadal trends of vertical stratification maximum and mixed layer properties. Trends inferred from Argo data for the period 2006–2020 for (**a**) vertical stratification maximum, (**b**) mixed layer depth, (**c**) mixed layer temperature and (**d**) mixed layer salinity. Trends are computed from the anomalies relative to the climatological seasonal cycle. Grey contour lines show the mean fields for the period of 2006–2020, respectively. Labels of the contour lines in (**a**) need to be multiplied by 10^{-3} to receive the squared Brunt-Väisälä frequency, N^2 [s^{-2}]. A positive trend of MLD refers to mixed layer deepening. Areas where the trend is not of 95% significance are stippled. Adapted from Roch et al. (2021)

the equatorial Kelvin wave activity that is an important driver of SST variability in the ABA (Imbol Koungue et al. 2017). In addition, the strong link between the fluctuations in the SAA strength and ABA SST (Lübbecke et al. 2010) has diminished since 2000. The Angola-Benguela region and the equatorial Atlantic are known to be strongly connected (Hu and Huang 2007; Illig et al. 2020; Lübbecke et al. 2010; Reason et al. 2006) and interannual SST variability has indeed also weakened along the equator. In particular, a 31% reduction of the interannual May–June–July SST variability was found in the eastern equatorial Atlantic (20°W-

Fig. 9.12 Weakening of interannual SST variability in the southeastern Atlantic. Difference of March–April–May SST anomalies standard deviation between 2000–2017 and 1982–1999 from ERA5. The blue shading depicts a reduction of the SST variability during 2000–2017 relative to 1982–1999. Adapted from Prigent et al. (2020a)
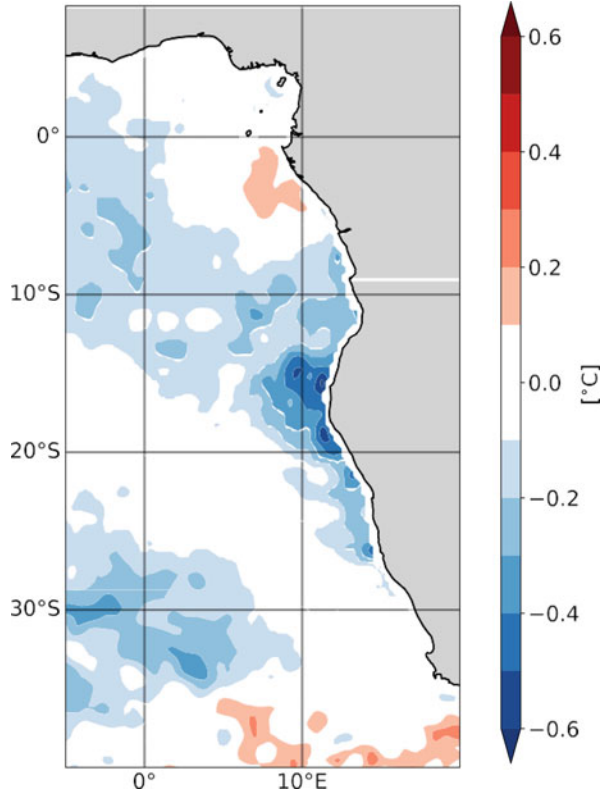
0°; 3°S-3°N) since 2000. The weakened SST variability in the eastern equatorial Atlantic was attributed to the reduced positive ocean-atmosphere feedback, the so-called Bjerknes feedback and increased thermal damping (Prigent et al. 2020b; Silva et al. 2021). Previously, Tokinaga and Xie (2011) reported a reduction of the eastern equatorial Atlantic variability over the period 1950–2009. They attributed the reduction in SST variability to a basin-wide warming, which is most pronounced in austral winter, reducing the annual cycle through positive ocean-atmosphere feedback.

The warming of the upper ocean during the recent decades is suggested to be the main reason for the ongoing deoxygenation of the ocean (Schmidtko et al. 2017). It is mainly attributed to a reduction of the oxygen solubility in warmer waters, but other mechanisms such as reduced subduction due to enhanced stratification or enhanced biological productivity might play a role as well (Oschlies et al. 2018). Downward oxygen trends and an expansion of the OMZ in the southeastern tropical Atlantic were first reported by Stramma et al. (2008). For the 100–500 m layer that include the core depth of the southeastern tropical Atlantic OMZ, available data for the period 1960 to 2010 predominantly suggests a deoxygenation in the southeastern Atlantic (Schmidtko et al. 2017). Oxygen reduction seems to be more confined to the

eastern boundary in the south. Near the ABFZ, oxygen concentrations might even increase (Fig. 9.10c). While the long-term oxygen trends (1960–2010) presented by Schmidtko et al. (2017) largely represent open-ocean conditions and are based on relatively sparse data coverage in the South Atlantic, Pitcher et al. (2021) found in 20-year oxygen time series taken at the shelf and continental slope off Walvis Bay, 23°S, no discernible deoxygenation trend. Along the southern Benguela coast Pitcher et al. (2014) reported no significant deoxygenation trend over the past 50 years as well, but an increase in the frequency of episodic anoxic events during recent years. The lack of long-term trends in dissolved oxygen concentrations on the shelf may be associated with the lack of significant phytoplankton biomass changes observed in this region (Lamont et al. 2019).

The general expectation is that long-term changes in upwelling-favorable winds, and hence the frequency and intensity of upwelling events, will result in variations in phytoplankton production and biomass on similar scales (Verheye et al. 2016), with related consequences for LOW formation and zooplankton biomass. However, to date, *in situ* and satellite observations have been unable to demonstrate clear linkages between physical forcing and subsequent ecosystem responses. For the African Large Marine Ecosystems, Sweijd and Smit (2020) found a general warming around Africa varying between 0.1 and 0.4°C decade^{-1}, while trends in productivity are much more heterogeneous with a tendency of enhanced productivity in the nBUS and sBUS and reduced productivity in the ABFZ. Besides the long-term warming in the nBUS, decreases in upwelling-favorable winds have been observed (Jarre et al. 2015b). Additionally, Lamont et al. (2018) reported substantially less upwelling-favorable wind in the nBUS since 2009, with a tendency toward fewer upwelling days and an increase in the number of events as upwelling has become less continuous. In contrast, the sBUS has shown a tendency toward increased upwelling and hence, long-term cooling (Lamont et al. 2018; Rouault et al. 2010). Annual to multidecadal variations in upwelling have been associated with shifts in the magnitude and position of the SAA, which drives upwelling-favorable winds in the region. Southward shifts of the SAA (Jarre et al. 2015b) appear to be responsible for the increased upwelling in the sBUS, with concomitantly less upwelling in the northern nBUS. Generally increasing phytoplankton biomass levels appear to be associated with the overall reduction in upwelling, as well as reduced grazing pressure from zooplankton communities, on the northern Benguela shelf (Lamont et al. 2019). In contrast, in the sBUS, increases in phytoplankton biomass levels on the Agulhas Bank during summer seem to be related to elevated nutrient levels arising from the observed increase in upwelling-favorable winds. Generally, the correspondence between long-term changes in upwelling-favorable winds and phytoplankton biomass on the west coast of South Africa has been more variable, with clear seasonal differences (Lamont et al. 2019).

9.5 Summary, Discussion and Recommendation for the Future Observing System

In this chapter we have presented a general view of our current understanding of the physical drivers of the eastern boundary upwelling system of the South Atlantic. The first part presents a description of the mean and the seasonal cycle of the eastern boundary upwelling system with a focus on local wind and remote equatorial forcing, tidal mixing and eddies. The description of the climatological situation is followed by observational evidence of the interannual variability including extreme warm and cold events, i.e., Benguela Niños and Niñas, as well as fluctuations in the Agulhas leakage. Decadal and multidecadal changes that are evident in the available observational datasets might be associated with internal variability of the climate system or with ongoing climate change due to global warming. Here, we showed evidence of long-term warming particularly enhanced near the ABFZ, of ocean deoxygenation particularly in the region of the deep OMZ, and also a reduction in the interannual variability associated with long-term thermocline deepening and strengthening stratification.

The upwelling system is separated into three subsystems: (1) the seasonally varying, mixing-driven tAUS, (2) the permanently wind-driven nBUS and (3) the seasonally varying, wind-driven sBUS. Seasonal variations in the tAUS are dynamically driven via the propagation of equatorial and coastal trapped waves that are remotely forced in the equatorial Atlantic. When arriving in the tAUS, the dominantly semiannual, coastal trapped waves are associated with upward and downward movements of the thermocline. Primary and secondary upwelling seasons are then established during phases of elevated thermocline in July/August and December/January, respectively. The upward nutrient supply during phases of elevated thermocline and reduced upper-ocean stratification is induced by vertical mixing predominantly forced by internal tides generated at the continental slope and shelf edge. The resulting productivity maximum in August is found to be delayed by about a month relative to the upwelling wave phases (Fig. 9.4c).

The nBUS and sBUS are wind-driven upwelling systems with localized enhanced upwelling cells, i.e., the Kunene, Northern Namibian, Walvis Bay and Lüderitz cells. Both regions, the nBUS and the sBUS, can be differentiated by their seasonality: while the sBUS is characterized by a strong seasonal cycle with enhanced wind forcing in austral spring and summer, the nBUS is a permanent upwelling system. Both the alongshore winds and the cyclonic wind stress curl that is established by the offshore displacement of the BLLCJ and the resulting onshore weakening of the wind are important mechanisms of near-coastal upwelling. Besides the wind forcing, the sBUS is strongly impacted by the turbulence associated with the shedding of Agulhas rings, eddies and filaments.

The observational record generally shows a warming trend of the sea surface since the 1980s, which is strongest in the ABFZ. While there is mostly warming in the nBUS, temperature data from the sBUS also indicate local cooling trends (Fig. 9.10a, b). A differential behavior of near-coastal and open ocean SST under
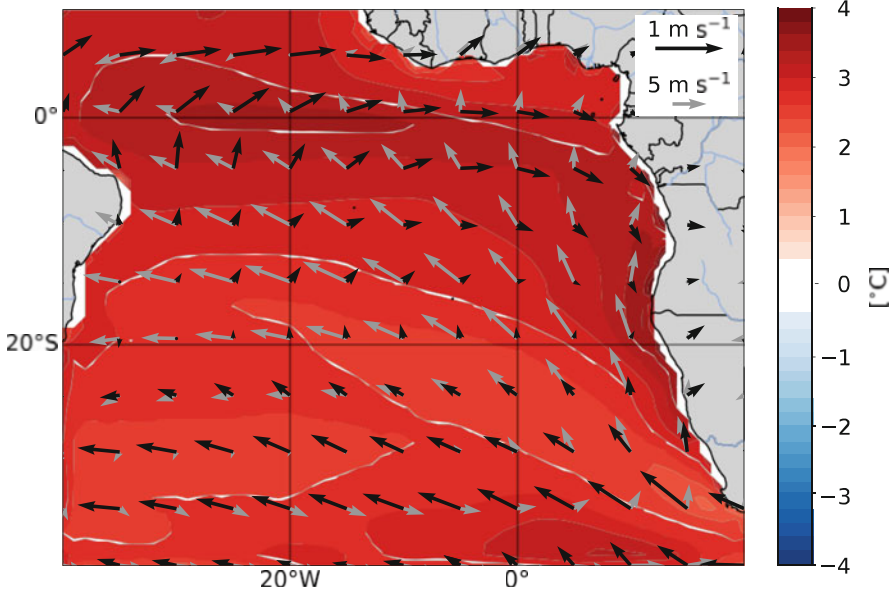
Fig. 9.13 Projected centennial sea surface temperature and wind changes in the South Atlantic. Difference of mean SST between 2070–2099 and 1970–1999 (shading) and difference of mean surface wind velocity between 2070–2099 and 1970–1999 (black arrows) from CMIP6 ensemble. CMIP6 ensemble mean surface wind velocity during 1970–1999 are shown as grey arrows. The CMIP6 ensemble is composed of 21 models. Prior to analysis the CMIP6 model data were interpolated on a common $1° \times 1°$ grid

climate warming was suggested by Bakun (1990) as a consequence of intensifying, upwelling-favorable winds due to increased air-temperature and sea-level pressure gradients between ocean and continent. To test this hypothesis, Sydeman et al. (2014) analyzed the available literature and found for the BUS evidence for a wind intensification only south of about 20°S. Such pattern, however, was found to be in general agreement with a southward shift of the SAA (Jarre et al. 2015b).

To further examine the mean SST response to sustained anthropogenic global warming, the worst-case scenario of the Shared Socioeconomic Pathway 5-8.5 (SSP5-8.5) applied to 21 General Circulation Models participating to the sixth phase of the Coupled Model Intercomparison Project (CMIP6) (Eyring et al. 2016) is used. Together with the equatorial Atlantic around 20°W, the Southwest African coast from 5°S to 30°S depicts the strongest warming (Fig. 9.13). Relative to 1970–1999, during 2070–2099 the SST in the region 0–10°S, 5–15°E (10–20°S; 5–15°E) is projected to increase by 3.2°C (3.3°C). In addition to the SST changes, the surface wind velocity field is also projected to change. Relative to 1970–1999, during 2070–2099, two major changes appear (Fig. 9.13): (1) the equatorial Atlantic easterly winds are found to decrease, (2) the southerly winds off Southwest Africa increase (decrease) south (north) of 20°S. The wind changes are in general agreement with

a southward shift of the SAA (Yang et al. 2020) leading to a weakening of the southerly, upwelling-favorable winds in the tAUS and the northern nBUS and strengthening winds in the southern nBUS and sBUS (Lima et al. 2019).

Differences in the driving mechanisms of the different regions, i.e., the tAUS, nBUS and sBUS, may result in different responses to future changes associated with climate warming. Projections for the tAUS indicate a further reduction of already weak upwelling-favorable winds. This region is likely more impacted by the warming and associated increase in stratification. A likely scenario includes a reduction of the thermocline response to remote equatorial forcing resulting in a weakening of seasonal and interannual variations. The prediction of corresponding changes of the marine ecosystem would require the understanding of the response of vertical mixing to temporal and spatial changes in the stratifications at the upper continental slope and shelves. The nutrient supply that fuels the primary productivity in the tAUS was suggested to be associated with vertical mixing induced dominantly by internal tides. It was found to be weaker for stronger stratification (Zeng et al. 2021), thus representing a possible mechanism how increased stratification in a warming climate might impact the marine ecosystem.

In accordance with a recent study by Wang et al. (2015), our results obtained from the analysis of the CMIP6 simulations suggest that the coastal upwelling will become more intense in the sBUS, while in the northern nBUS, similarly to the tAUS, upwelling-favorable winds are weakening. Wang et al. (2015) additionally suggested a change in the timing of upwelling with the upwelling season starting earlier and ending later at high latitudes (sBUS) and only weak changes at low latitudes (nBUS). This is also in agreement with a general poleward expansion of the tropics. Changes in the stratification suggest that a tropical stratification with fresh and warm surface waters expands southward into regions where surface waters are characterized by a salinity maximum (Roch et al. 2021).

While ocean warming and associated physical processes such as reduced oxygen solubility in seawater and reduced vertical exchange will be a dominant factor in expected future oxygen changes, low-oxygen regions in shallow waters on the shelf largely depend on the biological productivity and the related oxygen consumption. Here, strong interactions between physical and biological processes are expected but are not well understood for the present upwelling systems (Lamont et al. 2019). In general, current coupled physical–biogeochemistry–biological models do not reproduce observed patterns for oxygen changes in the ocean's thermocline making regional projections of future oxygen changes highly uncertain (Oschlies et al. 2018).

While CMIP6 climate models are improved compared to results from the previous phase, they still show substantial biases in the tropical Atlantic indicating the need for model improvements (Li et al. 2020; Richter and Tokinaga 2020). This is particularly the case when coupling physical, biogeochemical and ecosystem models. Improved understanding of physical processes, their interaction with the ecosystem and possible changes under climate warming relies on the availability of high-quality observations. Following the recommendations by Foltz et al. (2019)

made for the tropical Atlantic observing system, we suggest the following key points for the observing system at the eastern boundary of the South Atlantic:

1. The southeastern Atlantic particularly lacks a sustained observing system for the eastern boundary circulation and its variability associated with local and remote forcing. Subsurface moorings (shielded against fishing activity) and other advanced *in situ* platforms should be operated to obtain continuous time series at high temporal resolution to capture long-term changes in key parameters and to identify long-term changes in physical processes with enhanced short-term variability.
2. Observations of upper-ocean mixing using autonomous platforms such as moorings or gliders are required for estimates of vertical heat fluxes and upward nutrient supply. Turbulence observations must include simultaneous observations of stratification and velocity variability on short temporal scales. As vertical mixing will likely change under the impact of warming and increasing stratification, studying processes such as internal tides and waves, wind-generated near inertial waves, surface waves and other mixed layer processes on the shelf and at the continental slope will be of critical importance for the understanding of the future development of primary productivity.
3. As satellite data is often unavailable or uncertain in near-coastal regions the use of the full suite of ocean observations is recommended to fill the gaps. Particularly installing additional sensors for atmospheric and upper-ocean measurements on existing autonomous platforms such as drifters, sail-drones, wave-gliders, floats and gliders together with multidisciplinary research cruises is recommended.
4. Of critical importance will be the improvement of hindcast and forecast models as well as reanalysis products still showing large biases (Tchipalanga et al. 2018; Zuidema et al. 2016). This can be achieved by dedicated process studies to improve parameterizations of or to identify new processes in upwelling regions. Freely providing physical and biogeochemical data to open data centers to be used in assimilation systems and for the initialization of forecast models would be an important step to enhance the understanding of the mechanisms of upwelling variability and changes and to improve ocean predictions, which is crucially needed for the management of fisheries and the marine environment in the coastal areas of Southwest Africa.
5. Enhancing research capabilities in the coastal countries as well as international cooperation is a necessary condition to tackle challenges of ongoing climate change and climate variability.

References

Andrews WRH, Hutchings L (1980) Upwelling in the southern Benguela current. Prog Oceanogr 9:1–81. https://doi.org/10.1016/0079-6611(80)90015-4

Bachèlery ML, Illig S, Dadou I (2016) Interannual variability in the south-East Atlantic Ocean, focusing on the Benguela upwelling system: remote versus local forcing. J Geophys Res Oceans 121:284–310. https://doi.org/10.1002/2015jc011168

Bachèlery ML, Illig S, Rouault M (2020) Interannual coastal trapped waves in the Angola-Benguela upwelling system and Benguela Niño and Niña events. J Mar Syst 203:103262. https://doi.org/10.1016/j.jmarsys.2019.103262

Bakun A (1990) Global climate change and intensification of Coastal Ocean upwelling. Science 247:198–201. https://doi.org/10.1126/science.247.4939.198

Barange M, Pillar SC (1992) Cross-shelf circulation, zonation and maintenance mechanisms of Nyctiphanes-Capensis and Euphausia-Hanseni (Euphausiacea) in the northern Benguela upwelling system. Cont Shelf Res 12:1027–1042. https://doi.org/10.1016/0278-4343(92)90014-B

Bartholomae CH, van der Plas AK (2007) Towards the development of environmental indices for the Namibian shelf, with particular reference to fisheries management. Afr J Mar Sci 29:25–35. https://doi.org/10.2989/Ajms.2007.29.1.2.67

Beal LM, De Ruijter WPM, Biastoch A et al (2011) On the role of the Agulhas system in ocean circulation and climate. Nature 472:429–436. https://doi.org/10.1038/nature09983

Bettencourt JH, Lopez C, Hernandez-Garcia E (2012) Oceanic three-dimensional Lagrangian coherent structures: a study of a mesoscale eddy in the Benguela upwelling region. Ocean Model 51:73–83. https://doi.org/10.1016/j.ocemod.2012.04.004

Bordbar MH, Mohrholz V, Schmidt M (2021) The relation of wind-driven coastal and offshore upwelling in the Benguela upwelling system. J Phys Oceanogr 51:3117–3133. https://doi.org/10.1175/jpo-d-20-0297.1

Boyd AJ, Nelson G (1998) Variability of the Benguela current off the cape peninsula, South Africa. S Afr J Mar Sci Suid-Afrikaanse Tydskrif Vir Seewetenskap 19:27–39. https://doi.org/10.2989/025776198784126665

Boyer DC, Hampton I (2001) An overview of the living marine resources of Namibia. S Afr J Mar Sci Suid-Afrikaanse Tydskrif Vir Seewetenskap 23:5–35. https://doi.org/10.2989/025776101784528953

Brandt P, Bange HW, Banyte D et al (2015) On the role of circulation and mixing in the ventilation of oxygen minimum zones with a focus on the eastern tropical North Atlantic. Biogeosciences 12:489–512. https://doi.org/10.5194/bg-12-489-2015

Brandt P, Claus M, Greatbatch RJ et al (2016) Annual and semiannual cycle of equatorial Atlantic circulation associated with basin-mode resonance. J Phys Oceanogr 46:3011–3029. https://doi.org/10.1175/Jpo-D-15-0248.1

Bulgin CE, Merchant CJ, Ferreira D (2020) Tendencies, variability and persistence of sea surface temperature anomalies. Sci Rep 10:7986. https://doi.org/10.1038/s41598-020-64785-9

Capet X, McWilliams JC, Molemaker MJ et al (2008) Mesoscale to submesoscale transition in the California current system. Part II: frontal processes. J Phys Oceanogr 38:44–64. https://doi.org/10.1175/2007jpo3672.1

Chen ZY, Yan XH, Jo YH et al (2012) A study of Benguela upwelling system using different upwelling indices derived from remotely sensed data. Cont Shelf Res 45:27–33. https://doi.org/10.1016/j.csr.2012.05.013

Cockcroft AC (2001) Jasus lalandii 'walkouts' or mass strandings in South Africa during the 1990s: an overview. Mar Freshw Res 52:1085–1094. https://doi.org/10.1071/Mf01100

Demarcq H, Barlow R, Hutchings L (2007) Application of a chlorophyll index derived from satellite data to investigate the variability of phytoplankton in the Benguela ecosystem. Afr J Mar Sci 29:271–282. https://doi.org/10.2989/Ajms.2007.29.2.11.194

Desbruyères D, McDonagh EL, King BA et al (2017) Global and full-depth ocean temperature trends during the early twenty-first century from Argo and repeat hydrography (vol 30, pg 1985, 2017). J Clim 30:7577–7577. https://doi.org/10.1175/Jcli-D-17-0181.1

Djakouré S, Penven P, Bourlès B et al (2017) Respective roles of the Guinea current and local winds on the coastal upwelling in the northern gulf of Guinea. J Phys Oceanogr 47:1367–1387. https://doi.org/10.1175/Jpo-D-16-0126.1

Dufois F, Rouault M (2012) Sea surface temperature in False Bay (South Africa): towards a better understanding of its seasonal and inter-annual variability. Cont Shelf Res 43:24–35. https://doi.org/10.1016/j.csr.2012.04.009

Duncombe Rae CM (2005) A demonstration of the hydrographic partition of the Benguela upwelling ecosystem at 26°40′S. Afr J Mar Sci 27:617–628. https://doi.org/10.2989/18142320509504122

Eyring V, Bony S, Meehl GA et al (2016) Overview of the coupled model Intercomparison project phase 6 (CMIP6) experimental design and organization. Geosci Model Dev 9:1937–1958. https://doi.org/10.5194/gmd-9-1937-2016

Fennel W (1999) Theory of the Benguela upwelling system. J Phys Oceanogr 29:177–190. https://doi.org/10.1175/1520-0485(1999)029<0177:TOTBUS>2.0.CO;2

Fennel W, Junker T, Schmidt M et al (2012) Response of the Benguela upwelling systems to spatial variations in the wind stress. Cont Shelf Res 45:65–77. https://doi.org/10.1016/j.csr.2012.06.004

Florenchie P, Lutjeharms JRE, Reason CJC et al (2003) The source of Benguela Niños in the South Atlantic Ocean. Geophys Res Lett 30:1505. https://doi.org/10.1029/2003gl017172

Florenchie P, Reason CJC, Lutjeharms JRE et al (2004) Evolution of interannual warm and cold events in the Southeast Atlantic Ocean. J Clim 17:2318–2334. https://doi.org/10.1175/1520-0442(2004)017<2318:EOIWAC>2.0.CO;2

Flynn RF, Granger J, Veitch JA et al (2020) On-shelf nutrient trapping enhances the fertility of the southern Benguela upwelling system. J Geophys Res Oceans 125:e2019JC015948. https://doi.org/10.1029/2019JC015948

Foltz GR, Brandt P, Richter I et al (2019) The tropical Atlantic observing system. Front Mar Sci 6:206. https://doi.org/10.3389/fmars.2019.00206

Gammelsrød T, Bartholomae CH, Boyer DC et al (1998) Intrusion of warm surface water along the Angolan-Namibian coast in February-march 1995: the 1995 Benguela Niño. S Afr J Mar Sci Suid-Afrikaanse Tydskrif Vir Seewetenskap 19:41–56. https://doi.org/10.2989/025776198784126719

Gruber N (2011) Warming up, turning sour, losing breath: ocean biogeochemistry under global change. Philos Trans Royal Soc A-Math Phys Eng Sci 369:1980–1996. https://doi.org/10.1098/rsta.2011.0003

Gruber N, Lachkar Z, Frenzel H et al (2011) Eddy-induced reduction of biological production in eastern boundary upwelling systems. Nat Geosci 4:787–792. https://doi.org/10.1038/Ngeo1273

Hall C, Lutjeharms JRE (2011) Cyclonic eddies identified in the Cape Basin of the South Atlantic Ocean. J Mar Syst 85:1–10. https://doi.org/10.1016/j.jmarsys.2010.10.003

Herbert G, Bourlès B, Penven P et al (2016) New insights on the upper layer circulation north of the Gulf of Guinea. J Geophys Res Oceans 121:6793–6815. https://doi.org/10.1002/2016jc011959

Hersbach H, Bell B, Berrisford P, Hirahara S et al (2020) The ERA5 global reanalysis. Q J R Meteorol Soc 146:1999–2049. https://doi.org/10.1002/qj.3803

Hopkins J, Lucas M, Dufau C et al (2013) Detection and variability of The Congo River plume from satellite derived sea surface temperature, salinity, ocean colour and sea level. Remote Sens Environ 139:365–385. https://doi.org/10.1016/j.rse.2013.08.015

Hösen E, Möller J, Jochumsen K et al (2016) Scales and properties of cold filaments in the Benguela upwelling system off Luderitz. J Geophys Res Oceans 121:1896–1913. https://doi.org/10.1002/2015jc011411

Hu ZZ, Huang B (2007) Physical processes associated with the tropical Atlantic SST gradient during the anomalous evolution in the southeastern ocean. J Clim 20:3366–3378. https://doi.org/10.1175/Jcli4189.1

Hutchings L, Barange M, Bloomer SF et al (1998) Multiple factors affecting south African anchovy recruitment in the spawning, transport and nursery areas. S Afr J Mar Sci Suid-Afrikaanse Tydskrif Vir Seewetenskap 19:211–225. https://doi.org/10.2989/025776198784126908

Hutchings L, van der Lingen CD, Shannon LJ et al (2009) The Benguela current: an ecosystem of four components. Prog Oceanogr 83:15–32. https://doi.org/10.1016/j.pocean.2009.07.046

Illig S, Bachèlery ML, Cadier E (2018) Subseasonal coastal-trapped wave propagations in the southeastern Pacific and Atlantic oceans: 2. Wave characteristics and connection with the equatorial variability. J Geophys Res Oceans 123:3942–3961. https://doi.org/10.1029/2017jc013540

Illig S, Bachèlery ML, Lübbecke JF (2020) Why Do Benguela Niños Lead Atlantic Niños? J Geophys Res Oceans 125:e2019JC016003. https://doi.org/10.1029/2019JC016003

Imbol Koungue RA, Brandt P (2021) Impact of Intraseasonal waves on Angolan warm and cold events. J Geophys Res Oceans 126:e2020JC017088. https://doi.org/10.1029/2020JC017088

Imbol Koungue RA, Illig S, Rouault M (2017) Role of interannual kelvin wave propagations in the equatorial Atlantic on the Angola Benguela current system. J Geophys Res Oceans 122:4685–4703. https://doi.org/10.1002/2016jc012463

Imbol Koungue RA, Rouault M, Illig S et al (2019) Benguela Niños and Benguela Niñas in Forced Ocean simulation from 1958 to 2015. J Geophys Res Oceans 124:5923–5951. https://doi.org/10.1029/2019jc015013

Imbol Koungue RA, Brandt P, Lübbecke J et al (2021) The 2019 Benguela Niño. Front Mar Sci 8:800103. https://doi.org/10.3389/fmars.2021.800103

Jarre A, Hutchings L, Crichton M et al (2015a) Oxygen-depleted bottom waters along the west coast of South Africa, 1950-2011. Fish Oceanogr 24:56–73. https://doi.org/10.1111/fog.12076

Jarre A, Hutchings L, Kirkman SP et al (2015b) Synthesis: climate effects on biodiversity, abundance and distribution of marine organisms in the Benguela. Fish Oceanogr 24:122–149. https://doi.org/10.1111/fog.12086

Johns WE, Brandt P, Bourlès B et al (2014) Zonal structure and seasonal variability of the Atlantic Equatorial Undercurrent. Clim Dyn 43:3047–3069. https://doi.org/10.1007/s00382-014-2136-2

Johnson AS, Nelson G (1999) Ekman estimates of upwelling at cape columbine based on measurements of longshore wind from a 35-year time-series. S Afr J Mar Sci Suid-Afrikaanse Tydskrif Vir Seewetenskap 21:433–436. https://doi.org/10.2989/025776199784125971

Junker T, Schmidt M, Mohrholz V (2015) The relation of wind stress curl and meridional transport in the Benguela upwelling system. J Mar Syst 143:1–6. https://doi.org/10.1016/j.jmarsys.2014.10.006

Junker T, Mohrholz V, Siegfried L et al (2017) Seasonal to interannual variability of water mass characteristics and currents on the Namibian shelf. J Mar Syst 165:36–46. https://doi.org/10.1016/j.jmarsys.2016.09.003

Junker T, Mohrholz V, Schmidt M et al (2019) Coastal trapped wave propagation along the southwest African shelf as revealed by moored observations. J Phys Oceanogr 49:851–866. https://doi.org/10.1175/Jpo-D-18-0046.1

Kainge P, Kirkman SP, Estevao V et al (2020) Fisheries yields, climate change, and ecosystem-based management of the Benguela current large marine ecosystem. Environ Dev 36:100567. https://doi.org/10.1016/j.envdev.2020.100567

Karstensen J, Stramma L, Visbeck M (2008) Oxygen minimum zones in the eastern tropical Atlantic and Pacific oceans. Prog Oceanogr 77:331–350. https://doi.org/10.1016/J.Pocean.2007.05.009

Kolodziejczyk N, Marin F, Bourlès B et al (2014) Seasonal variability of the equatorial undercurrent termination and associated salinity maximum in the Gulf of Guinea. Clim Dyn 43:3025–3046. https://doi.org/10.1007/s00382-014-2107-7

Kopte R, Brandt P, Dengler M et al (2017) The Angola current: flow and hydrographic characteristics as observed at 11°S. J Geophys Res Oceans 122:1177–1189. https://doi.org/10.1002/2016jc012374

Kopte R, Brandt P, Claus M et al (2018) Role of Equatorial Basin-mode resonance for the seasonal variability of the Angola current at 11°S. J Phys Oceanogr 48:261–281. https://doi.org/10.1175/Jpo-D-17-0111.1

Koseki S, Imbol Koungue RA (2021) Regional atmospheric response to the Benguela Niñas. Int J Climatol 41:E1483–E1497. https://doi.org/10.1002/joc.6782

Lamont T, Hutchings L, van den Berg MA et al (2015) Hydrographic variability in the St. Helena Bay region of the southern Benguela ecosystem. J Geophys Res Oceans 120:2920–2944. https://doi.org/10.1002/2014jc010619

Lamont T, Garcia-Reyes M, Bograd SJ et al (2018) Upwelling indices for comparative ecosystem studies: variability in the Benguela upwelling system. J Mar Syst 188:3–16. https://doi.org/10.1016/j.jmarsys.2017.05.007

Lamont T, Barlow RG, Brewin RJW (2019) Long-term trends in phytoplankton chlorophyll a and size structure in the Benguela upwelling system. J Geophys Res Oceans 124:1170–1195. https://doi.org/10.1029/2018jc014334

Lass HU, Mohrholz V (2008) On the interaction between the subtropical gyre and the subtropical cell on the shelf of the SE Atlantic. J Mar Syst 74:1–43. https://doi.org/10.1016/j.jmarsys.2007.09.008

Li XW, Bordbar MH, Latif M et al (2020) Monthly to seasonal prediction of tropical Atlantic Sea surface temperature with statistical models constructed from observations and data from the Kiel climate model. Clim Dyn 54:1829–1850. https://doi.org/10.1007/s00382-020-05140-6

Lima DCA, Soares PMM, Semedo A et al (2019) How will a warming climate affect the Benguela coastal low-level wind jet? J Geophys Res-Atmos 124:5010–5028. https://doi.org/10.1029/2018JD029574

Lübbecke JF, Böning CW, Keenlyside NS et al (2010) On the connection between Benguela and equatorial Atlantic Niños and the role of the South Atlantic anticyclone. J Geophys Res Oceans 115:C09015. https://doi.org/10.1029/2009jc005964

Lübbecke JF, Brandt P, Dengler M et al (2019) Causes and evolution of the southeastern tropical Atlantic warm event in early 2016. Clim Dyn 53:261–274. https://doi.org/10.1007/s00382-018-4582-8

Lutjeharms JRE, Stockton PL (1987) Kinematics of the upwelling front off southern-Africa. S Afr J Mar Sci Suid-Afrikaanse Tydskrif Vir Seewetenskap 5:35–49. https://doi.org/10.2989/025776187784522612

Luyten JR, Pedlosky J, Stommel H (1983) The ventilated thermocline. J Phys Oceanogr 13:292–309. https://doi.org/10.1175/1520-0485(1983)013<0292:TVT>2.0.CO;2

Matthews SG, Pitcher GC (1996) Worst recorded marine mortality on the south African coast. In: Yasumoto T, Oshima Y, Fukuyo Y (eds) Harmful and toxic algal blooms. Intergovernmental Oceanographic Commission of UNESCO, Sendai, Japan, pp 89–91

Mohrholz V, Bartholomae CH, van der Plas AK et al (2008) The seasonal variability of the northern Benguela undercurrent and its relation to the oxygen budget on the shelf. Cont Shelf Res 28:424–441. https://doi.org/10.1016/j.csr.2007.10.001

Monteiro PMS, van der Plas AK (2006) Low Oxygen Water (LOW) variability in the Benguela system: key processes and forcing scales relevant to forecasting. In: Shannon V, Hempel G, Malanotte-Rizzoli P et al (eds) Large marine ecosystems. Elsevier, Amsterdam, pp 71–90. https://doi.org/10.1016/S1570-0461(06)80010-8

Monteiro PMS, van der Plas A, Mohrholz V et al (2006) Variability of natural hypoxia and methane in a coastal upwelling system: oceanic physics or shelf biology? Geophys Res Lett 33:L16614. https://doi.org/10.1029/2006gl026234

Monteiro PMS, van der Plas AK, Melice JL et al (2008) Interannual hypoxia variability in a coastal upwelling system: ocean-shelf exchange, climate and ecosystem-state implications. Deep-Sea Res I Ocean Res Pap 55:435–450. https://doi.org/10.1016/j.dsr.2007.12.010

Muller AA, Mohrholz V, Schmidt M (2013) The circulation dynamics associated with a northern Benguela upwelling filament during October 2010. Cont Shelf Res 63:59–68. https://doi.org/10.1016/j.csr.2013.04.037

NASA Goddard Space Flight Center (2018) Moderate-resolution Imaging Spectroradiometer (MODIS) Aqua Chlorophyll Data, 2018: Reprocessing. NASA OB.DAAC. https://doi.org/10.5067/AQUA/MODIS/L3B/CHL/2018. Accessed 20 Feb 2019

Nelson G (1989) Poleward motion in the Benguela area. In: Neshyba SJ, Mooers CNK, Smith RL et al (eds) Poleward flows along Eastern Ocean boundaries. Springer, New York, NY, pp 110–130. https://doi.org/10.1007/978-1-4613-8963-7_10

Nelson G, Hutchings L (1983) The Benguela upwelling area. Prog Oceanogr 12:333–356. https://doi.org/10.1016/0079-6611(83)90013-7

Oschlies A, Brandt P, Stramma L et al (2018) Drivers and mechanisms of ocean deoxygenation. Nat Geosci 11:467–473. https://doi.org/10.1038/s41561-018-0152-2

Ostrowski M, da Silva JCB, Bazik-Sangolay B (2009) The response of sound scatterers to El Niño- and La Niña-like oceanographic regimes in the southeastern Atlantic. Ices J Mar Sci 66:1063–1072. https://doi.org/10.1093/icesjms/fsp102

Patricola CM, Chang P (2017) Structure and dynamics of the Benguela low-level coastal jet. Clim Dyn 49:2765–2788. https://doi.org/10.1007/s00382-016-3479-7

Penven P, Roy C, de Verdiere AC et al (2000) Simulation of a coastal jet retention process using a barotropic model. Oceanologica Acta 23:615–634. https://doi.org/10.1016/S0399-1784(00)01106-3

Pitcher GC, Nelson G (2006) Characteristics of the surface boundary layer important to the development of red tide on the southern Namaqua shelf of the Benguela upwelling system. Limnol Oceanogr 51:2660–2674. https://doi.org/10.4319/lo.2006.51.6.2660

Pitcher GC, Probyn TA (2017) Seasonal and sub-seasonal oxygen and nutrient fluctuations in an embayment of an eastern boundary upwelling system: St Helena bay. Afr J Mar Sci 39:95–110. https://doi.org/10.2989/1814232x.2017.1305989

Pitcher GC, Probyn TA, du Randt A et al (2014) Dynamics of oxygen depletion in the nearshore of a coastal embayment of the southern Benguela upwelling system. J Geophys Res Oceans 119:2183–2200. https://doi.org/10.1002/2013jc009443

Pitcher GC, Aguirre-Velarde A, Breitburg D et al (2021) System controls of coastal and open ocean oxygen depletion. Prog Oceanogr 197:102613. https://doi.org/10.1016/j.pocean.2021.102613

Polo I, Lazar A, Rodriguez-Fonseca B et al (2008) Oceanic kelvin waves and tropical Atlantic intraseasonal variability: 1. Kelvin wave characterization. J Geophys Res Oceans 113:C07009. https://doi.org/10.1029/2007jc004495

Prigent A, Imbol Koungue RA, Lübbecke JF et al (2020a) Origin of weakened Interannual Sea surface temperature variability in the southeastern tropical Atlantic Ocean. Geophys Res Lett 47:e2020GL089348. https://doi.org/10.1029/2020GL089348

Prigent A, Lübbecke JF, Bayr T et al (2020b) Weakened SST variability in the tropical Atlantic Ocean since 2000. Clim Dyn 54:2731–2744. https://doi.org/10.1007/s00382-020-05138-0

Reason CJC, Smart S (2015) Tropical south East Atlantic warm events and associated rainfall anomalies over southern Africa. Front Environ Sci 3:24. https://doi.org/10.3389/fenvs.2015.00024

Reason CJC, Florenchie P, Rouault M et al (2006) 10 Influences of large scale climate modes and agulhas system variability on the BCLME region. In: Shannon V, Hempel G, Malanotte-Rizzoli P et al (eds) Large marine ecosystems. Elsevier, Amsterdam, pp 223–238. https://doi.org/10.1016/S1570-0461(06)80015-7

Ricciardulli L, Wentz FJ (2016) Remote sensing systems ASCAT C-2015 daily ocean vector winds on 0.25 deg grid, version 02.1. Remote Sensing Systems. http://www.remss.com/missions/ascat. Accessed 1 June 2019

Richter I (2015) Climate model biases in the eastern tropical oceans: causes, impacts and ways forward. Wiley Interdisc Rev Climate Change 6:345–358. https://doi.org/10.1002/wcc.338

Richter I, Tokinaga H (2020) An overview of the performance of CMIP6 models in the tropical Atlantic: mean state, variability, and remote impacts. Clim Dyn 55:2579–2601. https://doi.org/10.1007/s00382-020-05409-w

Richter I, Behera SK, Masumoto Y et al (2010) On the triggering of Benguela Niños: remote equatorial versus local influences. Geophys Res Lett 37:L20604. https://doi.org/10.1029/2010gl044461

Rixen T, Lahajnar N, Lamont T et al (2021) Oxygen and nutrient trapping in the southern Benguela upwelling system. Front Mar Sci 8:730591. https://doi.org/10.3389/fmars.2021.730591

Roch M, Brandt P, Schmidtko S et al (2021) Southeastern tropical Atlantic changing from subtropical to tropical conditions. Front Mar Sci 8:748383. https://doi.org/10.3389/fmars.2021.748383

Roemmich D, Church J, Gilson J et al (2015) Unabated planetary warming and its ocean structure since 2006. Nat Clim Chang 5:240–245. https://doi.org/10.1038/Nclimate2513

Rossi V, Lopez C, Sudre J et al (2008) Comparative study of mixing and biological activity of the Benguela and canary upwelling systems. Geophys Res Lett 35:L11602. https://doi.org/10.1029/2008gl033610

Rouault M (2012) Bi-annual intrusion of tropical water in the northern Benguela upwelling. Geophys Res Lett 39:L12606. https://doi.org/10.1029/2012gl052099

Rouault M, Florenchie P, Fauchereau N et al (2003) South East tropical Atlantic warm events and southern African rainfall. Geophys Res Lett 30:8009. https://doi.org/10.1029/2002gl014840

Rouault M, Pohl B, Penven P (2010) Coastal oceanic climate change and variability from 1982 to 2009 around South Africa. Afr J Mar Sci 32:237–246. https://doi.org/10.2989/1814232x.2010.501563

Rouault M, Illig S, Lübbecke J et al (2018) Origin, development and demise of the 2010-2011 Benguela Niño. J Mar Syst 188:39–48. https://doi.org/10.1016/j.jmarsys.2017.07.007

Roy C, Weeks S, Rouault M et al (2001) Extreme oceanographic events recorded in the southern Benguela during the 1999-2000 summer season. S Afr J Sci 97:465–471

Roy C, van der Lingen CD, Coetzee JC et al (2007) Abrupt environmental shift associated with changes in the distribution of cape anchovy Engraulis encrasicolus spawners in the southern Benguela. Afr J Mar Sci 29:309–319. https://doi.org/10.2989/Ajms.2007.29.3.1.331

Rubio A, Blanke B, Speich S et al (2009) Mesoscale eddy activity in the southern Benguela upwelling system from satellite altimetry and model data. Prog Oceanogr 83:288–295. https://doi.org/10.1016/j.pocean.2009.07.029

Russo CS, Lamont T, Krug M (2021) Spatial and temporal variability of the Agulhas retroflection: observations from a new objective detection method. Remote Sens Environ 253:112239. https://doi.org/10.1016/j.rse.2020.112239

Scannell HA, McPhaden MJ (2018) Seasonal mixed layer temperature balance in the southeastern tropical Atlantic. J Geophys Res Oceans 123:5557–5570. https://doi.org/10.1029/2018jc014099

Schmidt M, Eggert A (2016) Oxygen cycling in the northern Benguela upwelling system: modelling oxygen sources and sinks. Prog Oceanogr 149:145–173. https://doi.org/10.1016/j.pocean.2016.09.004

Schmidtko S, Stramma L, Visbeck M (2017) Decline in global oceanic oxygen content during the past five decades. Nature 542:335–339. https://doi.org/10.1038/nature21399

Sena Martins M, Stammer D (2022) Interannual variability of The Congo River plume-Induced Sea surface salinity. Remote Sens 14:1013. https://doi.org/10.3390/rs14041013

Shannon LV (1985) The Benguela ecosystem. Part I. evolution of the Benguela, physical features and processes. Oceanogr Mar Biol 23:105–182

Shannon LV, Nelson G (1996) The Benguela: large scale features and processes and system variability. In: Wefer G, Berger WH, Siedler G et al (eds) The South Atlantic: present and past circulation. Springer, Berlin, Heidelberg, pp 163–210. https://doi.org/10.1007/978-3-642-80353-6_9

Shannon LV, Boyd AJ, Brundrit GB et al (1986) On the existence of an El-Niño-type phenomenon in the Benguela system. J Mar Res 44:495–520. https://doi.org/10.1357/002224086788403105

Shannon LV, Agenbag JJ, Buys MEL (1987) Large-scale and mesoscale features of the Angola-Benguela front. S Afr J Mar Sci Suid-Afrikaanse Tydskrif Vir Seewetenskap 5:11–34

Siegfried L, Schmidt M, Mohrholz V et al (2019) The tropical-subtropical coupling in the Southeast Atlantic from the perspective of the northern Benguela upwelling system. PLoS One 14:e0210083. https://doi.org/10.1371/journal.pone.0210083

Silva P, Wainer I, Khodri M (2021) Changes in the equatorial mode of the tropical Atlantic in terms of the Bjerknes feedback index. Clim Dyn 56:3005–3024. https://doi.org/10.1007/s00382-021-05627-w

Small RJ, Curchitser E, Hedstrom K et al (2015) The Benguela upwelling system: quantifying the sensitivity to resolution and coastal wind representation in a global climate model. J Clim 28:9409–9432. https://doi.org/10.1175/Jcli-D-15-0192.1

Stramma L, Johnson GC, Sprintall J et al (2008) Expanding oxygen-minimum zones in the tropical oceans. Science 320:655–658. https://doi.org/10.1126/Science.1153847

Sun XM, Vizy EK, Cook KH (2019) Land-atmosphere-ocean interactions in the southeastern Atlantic: interannual variability. Clim Dyn 52:539–561. https://doi.org/10.1007/s00382-018-4155-x

Sweijd NA, Smit AJ (2020) Trends in sea surface temperature and chlorophyll-a in the seven African large marine ecosystems. Environ Dev 36:100585. https://doi.org/10.1016/j.envdev.2020.100585

Sydeman WJ, Garcia-Reyes M, Schoeman DS et al (2014) Climate change and wind intensification in coastal upwelling ecosystems. Science 345:77–80. https://doi.org/10.1126/science.1251635

Taunton-Clark J (1985) The formation, growth and decay of upwelling tongues in response to the mesoscale wind field during summer. In: Shannon LV (ed) South African Ocean colour and upwelling experiment. Sea Fisheries Research Institute, Cape Town (South Africa), pp 47–61

Tchipalanga P, Dengler M, Brandt P et al (2018) Eastern boundary circulation and hydrography off Angola: building Angolan oceanographic capacities. Bull Am Meteorol Soc 99:1589–1605. https://doi.org/10.1175/Bams-D-17-0197.1

Tokinaga H, Xie SP (2011) Weakening of the equatorial Atlantic cold tongue over the past six decades. Nat Geosci 4:222–226. https://doi.org/10.1038/Ngeo1078

Veitch JA, Penven P (2017) The role of the Agulhas in the Benguela current system: a numerical modeling approach. J Geophys Res Oceans 122:3375–3393. https://doi.org/10.1002/2016jc012247

Veitch J, Penven P, Shillington F (2009) The Benguela: a laboratory for comparative modeling studies. Prog Oceanogr 83:296–302. https://doi.org/10.1016/j.pocean.2009.07.008

Veitch J, Penven P, Shillington F (2010) Modeling equilibrium dynamics of the Benguela current system. J Phys Oceanogr 40:1942–1964. https://doi.org/10.1175/2010jpo4382.1

Veitch J, Hermes J, Lamont T et al (2018) Shelf-edge jet currents in the southern Benguela: a modelling approach. J Mar Syst 188:27–38. https://doi.org/10.1016/j.jmarsys.2017.09.003

Verheye HM, Lamont T, Huggett JA et al (2016) Plankton productivity of the Benguela current large marine ecosystem (BCLME). Environ Dev 17:75–92. https://doi.org/10.1016/j.envdev.2015.07.011

Vizy EK, Cook KH (2016) Understanding long-term (1982-2013) multi-decadal change in the equatorial and subtropical South Atlantic climate. Clim Dyn 46:2087–2113. https://doi.org/10.1007/s00382-015-2691-1

Vizy EK, Cook KH, Sun XM (2018) Decadal change of the South Atlantic Ocean Angola-Benguela frontal zone since 1980. Clim Dyn 51:3251–3273. https://doi.org/10.1007/s00382-018-4077-7

Wacongne S, Piton B (1992) The near-surface circulation in the northeastern corner of the South-Atlantic Ocean. Deep-Sea Res Part a-Oceanographic Research Papers 39:1273–1298. https://doi.org/10.1016/0198-0149(92)90069-6

Wang DW, Gouhier TC, Menge BA et al (2015) Intensification and spatial homogenization of coastal upwelling under climate change. Nature 518:390–394. https://doi.org/10.1038/nature14235

Wattenberg H (1929) Die Durchlüftung des Atlantischen Ozeans: (Vorläufige Mitteilung aus den Ergebnissen der Deutschen Atlantischen Expedition). ICES J Mar Sci 4:68–79. https://doi.org/10.1093/icesjms/4.1.68

Yang H, Lohmann G, Krebs-Kanzow U et al (2020) Poleward shift of the Major Ocean gyres detected in a warming climate. Geophys Res Lett 47:e2019GL085868. https://doi.org/10.1029/2019GL085868

Zeng Z, Brandt P, Lamb KG et al (2021) Three-dimensional numerical simulations of internal tides in the Angolan upwelling region. J Geophys Res Oceans 126:e2020JC016460. https://doi.org/10.1029/2020JC016460

Zuidema P, Chang P, Medeiros B et al (2016) Challenges and prospects for reducing coupled climate model SST biases in the eastern tropical Atlantic and Pacific oceans: the U.S. CLIVAR eastern tropical oceans synthesis working group. Bull Am Meteorol Soc 97:2305–2327. https://doi.org/10.1175/Bams-D-15-00274.1